

NASA TECHNICAL NOTE



NASA TN D-6343

C.1

NASA TN D-6343



**LOAN COPY: RETUR
AFWL (DOGL)
KIRTLAND AFB, N.**

**MIDCOURSE AND APPROACH GUIDANCE
REQUIREMENTS FOR SIMPLIFIED ONBOARD
CONTROL OF MOON-TO-EARTH TRAJECTORIES**

by Harold A. Hamer and Katherine G. Johnson

Langley Research Center

Hampton, Va. 23365



0132871

1. Report No. NASA TN D-6343		2. Government Accession No.		3. Recipi 0132871	
4. Title and Subtitle MIDCOURSE AND APPROACH GUIDANCE REQUIREMENTS FOR SIMPLIFIED ONBOARD CONTROL OF MOON-TO-EARTH TRAJECTORIES				5. Report Date July 1971	
				6. Performing Organization Code	
7. Author(s) Harold A. Hamer and Katherine G. Johnson				8. Performing Organization Report No. L-7662	
9. Performing Organization Name and Address NASA Langley Research Center Hampton, Va. 23365				10. Work Unit No. 110-06-05-06	
				11. Contract or Grant No.	
12. Sponsoring Agency Name and Address National Aeronautics and Space Administration Washington, D.C. 20546				13. Type of Report and Period Covered Technical Note	
				14. Sponsoring Agency Code	
15. Supplementary Notes					
16. Abstract <p>Simplified procedures have been developed for midcourse and approach guidance of moon-to-earth trajectories. These procedures require only simple onboard calculations based on optical angular measurements and lead to guidance predictions sufficiently accurate for emergency control of entry angle. An error analysis has shown that with onboard midcourse guidance corrections, an entry corridor of $\pm 1^\circ$ can be easily attained regardless of the distance to earth. Without a midcourse correction, this corridor is attainable if the approach guidance correction is delayed to a time within about 8 hours of reaching the earth. The approach guidance procedure can be adapted also to control the trajectory from earth-based line-of-sight measurements.</p>					
17. Key Words (Suggested by Author(s)) Approach guidance Onboard navigation guidance Transearth trajectories			18. Distribution Statement Unclassified - Unlimited		
19. Security Classif. (of this report) Unclassified		20. Security Classif. (of this page) Unclassified		21. No. of Pages 57	22. Price* \$3.00



CONTENTS

	Page
SUMMARY	1
INTRODUCTION	1
SYMBOLS	2
BASIC METHOD	6
APPROACH GUIDANCE PROCEDURE	7
With Midcourse Guidance	7
Star selection	8
Guidance velocity requirements	10
Sensitivity of entry angle to guidance measurement	11
Without Midcourse Guidance	11
Star selection	11
Guidance velocity requirements	12
Sensitivity of entry angle to guidance measurement	12
APPROACH-GUIDANCE ACCURACY CHARACTERISTICS	13
Effect of Measurement Error	13
Effect of Approximation Error	15
Effect of Maneuvering Error	15
Combined Effect of Guidance Errors	16
With midcourse guidance	16
Without midcourse guidance	16
Maneuver time	16
CONCLUDING REMARKS	17
APPENDIX A – SOME NOTES ON FIXED-TIME-OF-ARRIVAL ONBOARD	
MIDCOURSE GUIDANCE FOR TRANSEARTH TRAJECTORIES	18
Accuracy Characteristics	19
Effect of star selection	19
Effect of transition-matrix theory	20
Velocity Requirements	21
APPENDIX B – ESTIMATION OF ONBOARD MIDCOURSE VELOCITY ERROR	22
APPENDIX C – VELOCITY REQUIREMENT FOR APPROACH GUIDANCE	23
REFERENCES	24
TABLES	25
FIGURES	28

MIDCOURSE AND APPROACH GUIDANCE REQUIREMENTS
FOR SIMPLIFIED ONBOARD CONTROL OF
MOON-TO-EARTH TRAJECTORIES

By Harold A. Hamer and Katherine G. Johnson
Langley Research Center

SUMMARY

Simplified methods have been developed for midcourse and approach guidance of moon-to-earth trajectories. The methods utilize precalculated data to a great extent and require only simple onboard calculations based on optical angular measurements. These methods lead to guidance predictions sufficiently accurate for emergency control of entry angle. The approach guidance procedure can be adapted also to control the trajectory from earth-based line-of-sight measurements.

An error analysis, for which a 10-second-of-arc measurement error and a 0.2-m/sec maneuvering error were assumed, has shown that an entry corridor of $\pm 1^\circ$ can be generally attained by use of approach guidance, with or without onboard midcourse guidance. Including the midcourse guidance correction insures higher accuracy at entry. The effects of measurement-star location and approximation errors on the guidance accuracy are discussed also.

INTRODUCTION

In lunar missions navigation and guidance is normally accomplished by automatic procedures, which employ earth-based radar measurements. The inclusion of backup procedures which utilize onboard measurements is a desirable feature for emergency conditions which could occur during manned flights, such as failure in the radar system or loss of communications.

In previous years various onboard guidance procedures have been developed for controlling moon-to-earth trajectories. (For example, see refs. 1 and 2.) Error analyses have shown these procedures to be sufficiently accurate; however, they generally require repeated optical measurements and a number of guidance maneuvers. The procedures presented herein differ in that the guidance correction is determined from a single onboard position fix made at a preselected time. When used in conjunction with certain

approximations derived from two-body theory, this position fix is adequate for either midcourse or approach guidance and uses a single guidance maneuver in each case.

The guidance procedures presented herein represent a continuation of the work published in reference 3, wherein simplified guidance procedures were applied to earth-to-moon trajectories. For the most part, this paper incorporates the terminal guidance method of reference 3 to control entry angle of moon-to-earth trajectories. The method is employed as an approach guidance procedure either to refine the effects of transearth midcourse errors or to correct dispersions caused by transearth injection errors at the moon. In the latter case, no midcourse correction is made prior to the approach guidance correction. Similar measurements and guidance calculations are required for both cases, but there are differences in the accuracy characteristics and in the optimum measurement-star directions. A midcourse procedure which employs a fixed-time-of-arrival guidance law is also discussed, and some preliminary results are included.

The accuracy characteristics of the methods were determined by use of a Monte Carlo procedure. Spherically distributed injection errors at the moon were assumed in both the position and the velocity of the spacecraft. At midcourse, the error distribution was based on work done with translunar onboard midcourse guidance (ref. 4.). The standard Jet Propulsion Laboratory n-body trajectory program (ref. 5) was used to generate all trajectories required for the analysis.

SYMBOLS

A,B,C	matrices in midcourse-guidance equations (appendix A)
D	position deviation from nominal trajectory
D_I, D_{II}, D_{III}	position deviation in direction of star I, II, and III, respectively (appendix A)
δD	change in magnitude of D from $T_t = 9.5$ hours to $T_t = 10$ hours
ΔD	incremental value of position deviation
$E = r_e \cos \gamma_e$	
K, K_1, K_2, K_3	constants
l, m, n	direction cosine of line of sight to star with respect to X-, Y-, and Z-axis, respectively

R	earth radius
r	range to earth center
r_e	nominal entry range
r_l	range to moon center
Δr	incremental range to earth, $r_m - r_n$
Δr_l	difference from nominal range to moon (table II)
s	position deviation from nominal trajectory, $(\Delta x^2 + \Delta y^2 + \Delta z^2)^{1/2}$
T_e	time to nominal atmospheric entry time
T_p	time to nominal perilune time (table III)
T_{pf}	time of first midcourse position fix (appendix B)
T_t	time from transearth injection (perilune)
T_1	time of first midcourse guidance maneuver (appendix B)
Δt	difference from nominal entry time (table II)
u	velocity deviation from nominal trajectory, $(\Delta \dot{x}^2 + \Delta \dot{y}^2 + \Delta \dot{z}^2)^{1/2}$
V	spacecraft geocentric velocity
V_l	spacecraft selenocentric velocity
δV	difference from nominal geocentric velocity (table II)
δV_l	difference from nominal selenocentric velocity (table II)
ΔV	guidance velocity correction

X, Y, Z	rectangular right-hand axis system in which X-axis is in direction of Aries, XY-plane is parallel to earth equatorial plane, and Z-axis is in direction of celestial north pole
x, y, z	position coordinates in X, Y, Z system
$\Delta x, \Delta y, \Delta z$	off-nominal position component in direction of X-, Y-, and Z-axis, respectively – for example, $\Delta x = x_a - x_n$ (the notation $\langle \overline{\Delta x} \rangle$ represents the vector $\begin{pmatrix} \Delta x \\ \Delta y \\ \Delta z \end{pmatrix}$)
$\dot{x}, \dot{y}, \dot{z}$	velocity coordinates in X, Y, Z system
$\Delta \dot{x}, \Delta \dot{y}, \Delta \dot{z}$	off-nominal velocity component in direction of X-, Y-, and Z-axis, respectively – for example, $\Delta \dot{x} = \dot{x}_a - \dot{x}_n$
x_r, y_r, z_r	position coordinates in rotating Cartesian axis system in which X_r -axis lies along earth-moon line, $X_r Y_r$ -plane is in earth-moon plane, and Z_r -axis is in northerly direction
α	semisubtended angle
γ	flight-path angle at time of approach guidance
γ_e	flight-path angle at nominal entry altitude of 121.92 km (400 000 ft)
$\Delta \gamma_e$	incremental flight-path angle at nominal entry altitude, $\gamma_{e,a} - \gamma_{e,n}$
δ	angle formed at vehicle between line of sight to star and its projection in selenocentric orbital plane
θ	angle formed at vehicle by line of sight to star and line of sight to celestial-body center (referred to as star-to-body angle)
λ	angle between approach-guidance velocity vector and spacecraft velocity vector
μ	product of universal gravitational constant and mass of earth

σ standard deviation or root-mean-square value of error

σ_s standard deviation or root-mean-square value of s

σ_u standard deviation or root-mean-square value of u

$\begin{bmatrix} \Phi_1 \\ \Phi_2 \end{bmatrix}, \begin{bmatrix} \phi_1 \\ \phi_2 \end{bmatrix}$ submatrices in state-transition matrices (appendix B)

Subscripts:

a actual value

D position deviation

F first midcourse correction (appendix A)

inj transearth injection

m measured value

meas due to measurement error

n nominal value

R earth radius

r range to earth center

S second midcourse correction (appendix A)

$T_{,pf}$ at time of first midcourse position fix (appendixes A and B)

$T_{,1}$ at time of first midcourse guidance maneuver (appendix B)

ΔV guidance velocity

α semisubtended angle of earth

γ_e flight-path angle at nominal entry altitude

θ	star-to-body angle
1 to 6	specified directions

A bar over a symbol indicates a vector.

BASIC METHOD

Two guidance techniques are considered in the present analysis: An approach guidance procedure is discussed fully, and a fixed-time-of-arrival midcourse guidance procedure is given in appendix A. Each method yields a guidance correction from a single position fix, which is determined from deviations in preselected directions from a nominal trajectory. For the midcourse guidance correction, three deviations in the direction of each of three stars are required, inasmuch as the spacecraft is guided to a fixed point. The approach guidance correction requires the determination of only one deviation.

The geometry for the approach guidance method is shown in figure 1. The same variables are involved for the midcourse guidance. The deviation D of the actual trajectory from the nominal is normally determined by two onboard optical measurements: a star-to-body angle θ_m and a range measurement r_m . Range can be determined optically by measuring the angle subtended by the earth or by other measurements. (See ref. 4.) The corresponding nominal values would be known.

The nominal trajectory chosen for this paper is depicted in figure 2. The perilune is considered as the transearth injection point and has a radius of 3358 km. The selenocentric velocity is 1.992 km/sec; the time to earth atmospheric entry is 3.22 days. The nominal entry altitude selected was 121.92 km (400 000 ft).

From an equation derived in reference 3 for control of periapsis radius, a guidance velocity correction is developed from a closed-form expression relating entry and upstream conditions. These conditions are then related to deviations from a nominal trajectory, and a technique is developed to control the entry angle γ_e . Although not specifically designed to control the along-track and cross-track position errors at entry, the method adequately compensates for these errors.

For earth-approach trajectories, the substitution of the expression $E = r_e \cos \gamma_e$ in the aforementioned equation results in the following expression for correcting entry angle:

$$\Delta V = \frac{V \left[r^2 \cos \gamma \cos (\gamma + \lambda) - E_n^2 \cos \lambda \right]}{E_n^2 - r^2 \cos^2 (\gamma + \lambda)} \pm \frac{E_n \left\{ \left(r^2 - E_n^2 \right) V^2 \sin^2 \lambda + \left[r^2 \cos^2 (\gamma + \lambda) - E_n^2 \right] \left(\frac{2\mu}{r_e} - \frac{2\mu}{r} \right) \right\}^{1/2}}{E_n^2 - r^2 \cos^2 (\gamma + \lambda)} \quad (1)$$

The alternate signs of the second term correspond to correcting for either side of the earth. The sign which results in the lesser value of ΔV would ordinarily be chosen.

In equation (1), the flight-path angle γ has the major influence on the magnitude of ΔV for a given guidance pointing angle λ and guidance-maneuver time. It will be shown in subsequent figures that the value of γ is highly correlated with the deviation from the nominal trajectory in certain directions. Furthermore, it will be shown that a measurement star in one of these preselected directions can be used to obtain the deviation D , and hence the required value of ΔV .

APPROACH GUIDANCE PROCEDURE

Application of the approach guidance procedure in two different ways was studied. First, the approach guidance correction is applied after a transearth midcourse correction has been applied; second, the approach guidance correction is applied without prior midcourse correction. In essence, the first method corrects the approach trajectory for errors incurred at midcourse, the second corrects for errors incurred at the moon.

With Midcourse Guidance

It was assumed that a transearth first midcourse maneuver, employing the onboard method of reference 4, was performed about $20\frac{1}{2}$ hours from perilune. (See fig. 2.) By using results obtained with this method for translunar trajectories, it was established that the midcourse guidance error is due mainly to errors in the onboard measurements, rather than in maneuver execution, and that the dominant measurement errors and the position-determination errors are generally in the direction of the spacecraft velocity vector. Thus, the midcourse guidance error is essentially an error in the magnitude of ΔV rather than in its direction. The resulting error distribution yields an elongated ellipsoid with a 1σ error of about 1 m/sec in the midcourse velocity correction. The 1σ in-plane and out-of-plane errors in the direction of ΔV are 1.80° and 0.69° , respectively, where the reference plane is the nominal orbital plane of the spacecraft. For translunar trajectories, an error of 1 m/sec in midcourse ΔV resulted from a range-measurement error of about 20 km. (See ref. 4.) From the equations presented in

appendix B, it was determined that for transearth trajectories, an error of 1 m/sec in ΔV was induced by an error of 40 to 50 km in determining range.

By use of a Monte Carlo procedure, simulated midcourse errors were applied to the nominal trajectory to produce a number of perturbed trajectories. This method eliminates the calculation and application of both a first and a second midcourse correction. A second midcourse maneuver is inherent in fixed-time-of-arrival guidance, since it must correct the velocity error induced at the aim point by the derivation of the first midcourse velocity correction. Under actual operations, the approach-guidance measurements can be made only after a second midcourse correction has been applied.

Star selection.- The deviation D was determined by use of the relationship

$$D = l(x_a - x_n) + m(y_a - y_n) + n(z_a - z_n)$$

where l , m , and n , the direction cosines of the line of sight to the measurement star, are known. The measurement star is selected to yield the most effective direction for the deviation. Some of the directions for D which were investigated are illustrated in figure 3. Angles indicated represent attainable accuracies. The directions were chosen in two planes: the nominal orbital plane and the nominal instantaneous earth-moon-vehicle plane. At $T_e = 9$ hours, the angle between these planes is about 55° . Also, the spacecraft velocity vector \bar{V} is about 13° out of the earth-moon-vehicle plane. As indicated, $\overline{\Delta V}$ is generally preset 90° from the nominal velocity vector. The major axis of the position error ellipsoid, also indicated in the figure, lies within 1° of the orbital plane and was derived from errors incurred at first midcourse guidance. The deviation directions were chosen to essentially cover the entire spectrum of possible angles, as shown in figure 3(b). (The deviation D_6 is referenced to an earlier time $T_e = 9.4$ hours.)

The variation of deviation D with flight-path angle is shown in figures 4 to 7 for several directions of D and for several measurement times. Each data point represents the condition at the indicated time on a perturbed trajectory resulting from errors at first midcourse guidance. Small differences in values of flight-path angle at the time of the measurement are magnified considerably at entry if not corrected: Large γ values yield high g trajectories, whereas small values lead to trajectories which could skip out of or even miss the atmosphere.

The data in figures 4 to 7 show that with midcourse guidance included, the deviation D is a good prediction of γ . This relationship suggests that D can be used empirically to determine the guidance velocity correction because the ΔV required to change entry angle is dependent on the value of γ . (See eq. (1).) It will be shown that this dependence is not as great for trajectories in which midcourse guidance is not included.

The scatter of the data in figures 4 to 7 produces error in the guidance procedure. It is important that the amount of scatter be minimized by selecting the most effective direction for D . The similarity of scatter characteristics in figures 4 to 7 suggests that for the case in which a midcourse guidance correction has been previously applied, the direction of the deviation (star) and the time of measurement are not critical so far as approximation error is concerned. This contrasts with lunar-approach guidance where the direction of the star must be within 2° or 3° of a given plane. (See ref. 3.) For earth return, the trajectory position errors are concentrated along the major axis of the error ellipsoid (fig. 3); for example, at $T_e = 9$ hours, the length (1σ) of the major axis is 236 km compared with 9.4 km and 2 km for the other axes. Similarly, the velocity errors are almost entirely along the major axis of the velocity error ellipsoid, which is in the approximate direction of the earth.

It should be pointed out, however, that the deviation direction affects the measurement sensitivity which in turn affects the guidance accuracy attributable to measurement error. Comparison may be made between figures 4(b) and 7(a) where the deviations D_1 and D_3 are both perpendicular to the range vector but in a different plane. Choosing the deviation in the earth-moon-vehicle plane (fig. 7(a)) reduces the deviation (measurement) sensitivity considerably, and the reduced sensitivity increases the effect of measurement error.

The results in figures 5 and 6 show deviation directions which yield maximum sensitivity. Figure 6 gives the variation of flight-path angle with Δr , the difference between the nominal and measured range. The Δr values essentially indicate deviations measured directly toward (or away from) the center of the earth.

The deviation directions in figure 5 would lead to large measurement-error effects on guidance accuracy since $\theta_n \neq 90^\circ$, and even larger effects in figure 6 where $\theta_n = 0^\circ$. To minimize measurement error, the most suitable deviation direction is perpendicular to the nominal range vector, as shown in figures 4 and 7(a). These results are discussed in the section "Approach-Guidance Accuracy Characteristics." Figures 7(b) and 7(c) are included to give broader coverage of the entire spectrum of directions considered in the earth-moon-vehicle plane. (See also fig. 3(b).)

The foregoing results for approach guidance have been applied to the case in which midcourse guidance velocity errors are generally along the direction of the spacecraft velocity vector, the direction normally expected for onboard midcourse velocity errors. It is of interest to examine the effect on approach guidance of midcourse errors in other directions which might result from other midcourse procedures. Accordingly, midcourse velocity errors of the same magnitude and angular displacement previously used were applied normal to the spacecraft velocity vector in the orbital plane. The resulting data

are presented in figure 8. (Note the staggered vertical scale, which is read in such a manner that at $D = 0$, $\gamma = -73.954^\circ$.) Although a strong correlation between flight-path angle and certain directions of deviation D is shown, the range of effective directions was restricted. For example, the scatter for D_5 is considered unacceptable in that the maximum error in γ is $>0.01^\circ$. The deviations D_2 , D_3 , and D_4 , and Δr also exhibited excessive scatter, as well as low sensitivity, and are not shown. It is apparent that should the midcourse velocity errors be perpendicular to the spacecraft velocity vector, satisfactory deviations can be taken only in a limited range of directions. (See fig. 3(a).)

Guidance velocity requirements.- Characteristics of the approach guidance velocity are shown in figures 9 to 13. Figure 9 is an example of the variation of the velocity correction with the deviation D_3 . The positive and negative values of ΔV indicate $\lambda = \pm 90^\circ$. The circular symbols represent various trajectories perturbed at first midcourse guidance and were computed from the curve presented in figure 7(a) for $T_e = 9$ hours. Some data are also shown for two other times to indicate the general trend of the data. The offset in ΔV at $D_3 = 0$ (for each curve) is the results of two-body approximation (eq. (1)) and must be corrected by shifting the curves vertically to zero offset. After obtaining the value of the deviation, the astronaut uses a curve such as that shown in figure 9 to determine the required ΔV magnitude.

The calculations for ΔV are performed before flight and, as shown by equation (1), require the perturbed values of γ , r , and V at the measurement time, as well as the nominal value of $E = r_e \cos \gamma_e$. The ΔV values in figure 9 represent application of the thrust in the nominal orbital plane, perpendicular to the nominal velocity vector, the optimum direction for most times along the approach trajectory. (See fig. 10.)

Given in figure 10 are the magnitudes of ΔV required for correcting one particular perturbed trajectory; any other trajectory would have similar requirements percentage-wise. The astronaut uses this type of data to choose the time for the guidance maneuver. The data show that the ΔV requirement increases as the guidance maneuver is delayed to times closer to the earth. The value of the guidance pointing angle $\lambda = 90^\circ$ represents application of the ΔV vector perpendicular to the nominal velocity vector; the value $\lambda = 0^\circ$ represents application of the ΔV vector along the nominal velocity vector. The ΔV vector is always applied in the nominal orbital plane. It is evident that $\lambda = 90^\circ$ is essentially optimum for all times from entry. For $T_e = 4$, the optimum value is about 70° , but the use of $\lambda = 90^\circ$ results in a negligible increase in the ΔV requirements.

The results in figures 11 to 13 define the approach guidance velocity requirements. The symbols in figures 11 and 12, which correspond to the data of figure 9, have been shifted for zero offset. Note in figure 11 that only three of the 50 perturbed trajectories exceed the $\Delta\gamma_e$ value of $\pm 1^\circ$, and these by only a small amount. Thus with midcourse

guidance included, approach guidance becomes less important except when the midcourse error is not along the spacecraft velocity vector. In figure 8, where the error is essentially normal to the velocity vector, the magnitude of $\Delta\gamma_e$ exceeds $\pm 1^\circ$ two-thirds of the time. As will be discussed subsequently, data in the form shown in figure 11 are used to determine the effect of scatter (approximation) error and guidance velocity-cutoff error on entry-angle accuracy. Equivalent data are shown in figure 12. The ΔV values are shown as a function of $r_e \cos \gamma_e$ because this relationship can be calculated analytically from the derivative of equation (1). (See appendix C.) The calculated results and those obtained from the slopes of the curves in figure 12 coincide with the curve shown in figure 13. The curve shows the substantial increase in the guidance velocity requirement as the guidance maneuver is delayed to times closer to the earth. Obviously, the velocity-requirement ratio $\Delta(\Delta V)/\Delta(r_e \cos \gamma_e)$ can be readily converted to the more usable form $\Delta V/\Delta\gamma_e$ for error analysis.

Sensitivity of entry angle to guidance measurement.- Examples of the variation of deviation with incremental entry angle are shown in figure 14. This information is required for determining the effect of measurement error on the control of entry angle. The data are shown with respect to the deviation D_1 rather than D_3 since the effect of measurement error for the D_1 direction is smaller because of the increased sensitivity of D .

Without Midcourse Guidance

The approach guidance method discussed in this section corrects perturbed trajectories due to trajectory errors incurred at the moon and is the only guidance applied to the return trajectory. For the analysis, the Monte Carlo procedure was used to produce a number of perturbed trajectories emanating from perilune. The errors were essentially distributed spherically with 1σ values of about 2 km for position deviation s and about 2 m/sec for velocity deviation u . These errors could represent errors in the transearth injection for return to the earth.

Star selection.- Shown in figure 15 are examples of the variation of γ with D at $T_e = 9.4$ hours for two star directions. (Note the staggered scale, which is read in such a manner that at $D = 0$, $\gamma = -74.11^\circ$.) Except for the ranges covered, the data are similar to those shown in figures 4 to 7, where midcourse guidance was included. It is apparent that under certain conditions, the deviation D essentially predicts γ . However, as shown by figures 15 and 16, the deviation direction which gives the best correlation for γ is not the best for predicting the required approach correction ΔV .

The variation of ΔV with deviation is shown in figure 16 for the perturbed trajectories. This figure is similar to figure 9, except that certain perturbed trajectories do not enter the atmosphere if no ΔV correction is applied. The ΔV values in figure 16

were calculated from the actual γ values of figure 15. The rms value of ΔV shown for each set of data in figure 16 is the 1σ value of the scatter in the data about the line. This value is used in the subsequent error analysis as a measure of the amount of scatter (approximation) error. As indicated in figure 16, the measurement-star direction is of great importance in case of no midcourse guidance. In regard to scatter, the optimum direction of D at $T_e = 9.4$ hours corresponds to a star lying in the nominal orbital plane in a direction 77° from \bar{r}_n . (Note in fig. 3(a) that this direction is to the left of the earth.)

The variation of ΔV with D for the perturbed trajectories is shown in figure 17, for two values of θ_n at $T_e = 17.4$ hours. Here again, the 1σ values correspond to the scatter about the lines. (Note the staggered vertical scale, which is read in such a manner that at $D = 0$, $\Delta V = -0.6$ m/sec. The curves should be shifted vertically to correct for this zero offset.) For $T_e = 17.4$ hours, it is apparent from the scatter that the optimum direction of D corresponds to $\theta_n = 80^\circ$. Data are shown for $\theta_n = 90^\circ$ because no range measurement is required. Elimination of the range measurement is important from an operational standpoint, as well as for the fact that range-determination error is a dominant factor affecting the guidance measurement accuracy. The effect of the increase in scatter incurred by omitting the range measurement is discussed in the subsequent error analysis.

With regard to scatter error, the optimum direction of D at $T_e = 4.4$ hours is about 71° . It is of interest to note that since the true anomaly of the trajectory changes approximately 15° from $T_e = 17.4$ hours to $T_e = 4.4$ hours, the corresponding change in the optimum direction of the measurement star is 6° away from the earth. It should be noted also that for acceptable scatter, the nominal value selected for the star-to-body angle may lie within a region of several degrees in either the in-plane or out-of-plane direction.

Guidance velocity requirements.- The guidance velocity requirements, with respect to the deviation D , were discussed in the previous section in connection with selecting the optimum measurement star. In figure 18, ΔV is shown as a function of $\Delta\gamma_e$ for $T_e = 9.4$ hours, where the quantity $\Delta\gamma_e$ is the difference between the nominal and actual values of entry angle (at an altitude of 121.92 (400 000 feet)) for the various perturbed trajectories. The ΔV values are those given in figure 16 and are calculated values required to correct the $\Delta\gamma_e$ to zero. There are perturbed trajectories beyond the point $\Delta\gamma_e = 4^\circ$, but these do not enter the atmosphere. The sensitivity of ΔV with $\Delta\gamma_e$ at $\Delta\gamma_e = 0$ is utilized in the error analysis.

Sensitivity of entry angle to guidance measurement.- The values in figures 16(b) and 18 were cross plotted to obtain figure 19, which shows the variation of D_6 with $\Delta\gamma_e$. The value of the slope of this curve at $\Delta\gamma_e = 0$ is essential in determining the effect of

measurement error on guidance accuracy. Only the slope at $\Delta\gamma_e = 0$, that is at nominal γ_e , is required because all perturbed trajectories are corrected to the vicinity of $\Delta\gamma_e = 0$. It is of interest to note that the slope in figure 19 is about twice that for data where the trajectories were perturbed at first midcourse guidance (fig. 14). Absence of scatter in the data shown in figure 19 can also be used as a good indication for the optimum direction of D .

APPROACH-GUIDANCE ACCURACY CHARACTERISTICS

In this section, the more important errors associated with the approach guidance procedure are defined and analyzed. The analysis spans the region for performing the guidance from $T_e = 18$ hours to $T_e = 4$ hours. At $T_e = 18$ hours the spacecraft is about midway between the earth and moon. (See fig. 2.) Both procedures, that is, with and without midcourse guidance, are analyzed.

The approach guidance procedure is designed to control only the entry flight-path angle; however, the error analysis has shown that the along-track and cross-track positions are also controlled to a reasonable accuracy. For example, in the case with a midcourse guidance correction included, the approach guidance procedure reduced the 1σ position error at entry from 122 km to 17 km, these errors being almost entirely in the along-track direction. Similar results were obtained for the case without a midcourse guidance correction, except the uncorrected position errors at the earth were considerably higher.

Effect of Measurement Error

Error in the onboard optical measurements affects the approach-guidance accuracy. Error equations for such measurements were developed in reference 6. The equation used in this report is

$$\sigma_D = \left[(\cos \theta \sigma_r)^2 + (r \sin \theta \sigma_\theta)^2 \right]^{1/2} \quad (2)$$

which corresponds to uncorrelated errors in the measurement of range r and star-to-body angle θ . It is assumed that range is measured by α , the half-angle subtended by the earth at the spacecraft. The error σ_θ is constant at all values of time; whereas σ_r varies with time (or range) according to the relation given in reference 6,

$$\sigma_r = \left[\frac{r^2}{R^2} \left(\sigma_R^2 + r^2 \sigma_\alpha^2 \right) \right]^{1/2} \quad (3)$$

where σ_R is the uncertainty in defining the earth's radius and σ_α is constant. The variations of the nominal range and α with time are shown in figure 20.

In equation (2) nominal values for r and θ are used. For values of $\theta_n \approx 90^\circ$, it is seen that

$$\sigma_D \approx r\sigma_\theta$$

In this case, the range-measurement error is insignificant; hence, the nominal range value can replace the measured range in the equation given for D in figure 1. Because no range measurement is required, the approach method could be adapted to control the trajectory from earth-based line-of-sight measurements. If, for instance, a failure in the radar system prevented range and range-rate measurements, earth-based angular measurements could be substituted for star-to-body measurements. Even though relatively inaccurate, the angular measurements could be averaged over a period of time.

For $\theta_n \neq 90^\circ$, the effect of range-measurement error σ_r becomes important, as shown by equation (2). Figure 21 shows the variation with time of σ_r , the 1σ error in determining range from the α measurement. The data are shown both with and without consideration of the earth-radius uncertainty σ_R . The effect of excluding this uncertainty in the ensuing error analysis would be negligible. As shown by the other curve in the figure, it may be more accurate to use the nominal value instead of measuring the range at certain distances from the earth. This condition would, of course, depend upon the injection-error statistics at the moon. The curve was determined from normalized values obtained from the perturbed trajectories. The value of the injection-position error σ_S is given in the figure although its effect on σ_r is minor.

The effect of measurement error on the guidance accuracy is presented in figure 22 for approach guidance with and without a previous midcourse correction. The upper plot shows the variation of error in determining the deviation D with time from entry. These data were obtained by the use of equation (2) and the solid curve in figure 21. The sensitivity ratios shown in the middle plot of figure 22 are used to convert the σ_D data to the rms γ_e values shown in the lowest plot. Sensitivities were obtained from data such as those shown in figures 14 and 19. For the data with midcourse guidance, the sensitivity ratio is nearly constant with time since the overall magnitude of D does not change appreciably. (See figs. 16 and 17.)

The effect of errors in the range measurement is shown in the two curves in the upper plot of figure 22. The upper curve was calculated for the values of θ_n which correspond to minimum scatter. (For example, see figs. 16(b) and 17.) Since star direction is not critical for scatter in the case with midcourse guidance included, the lower

curve was calculated for $\theta_n = 90^\circ$, which is optimum with regard to measurement error. The deviation error is highly dependent on the value selected for θ_n . For instance, for D_2 , which corresponds to $\theta_n \approx 126.3^\circ$, σ_D at $T_e = 9$ hours would be about 55 km. If Δr were used as the guidance measurement, $\theta_n \approx 0^\circ$, (fig. 6), the value of σ_D would equal that of σ_r , which is about 90 km at that time. In these cases, however, the values of $\sigma_{\gamma,e}$ would not increase in the same proportion because the sensitivity ratio $\Delta\gamma_e/\Delta D$ would be about three times smaller in the case with midcourse guidance.

Effect of Approximation Error

The upper plot in figure 23 shows the effect of scatter (approximation) error on the accuracy of controlling entry angle. These curves were determined from

$$(\sigma_{\gamma,e})_{\text{scatter}} \approx (\sigma_{\Delta V})_{\text{scatter}} \left(\frac{\Delta\gamma_e}{\Delta V} \right) \quad (4)$$

where the value for $(\sigma_{\Delta V})_{\text{scatter}}$ was obtained from data such as those shown in figures 16 and 17. The ratio $\Delta\gamma_e/\Delta V$ is the reciprocal of the velocity-requirement ratio, which can be determined from figure 13 by use of the equation

$$\frac{\Delta V}{\Delta\gamma_e} = \frac{\Delta(\Delta V)}{\Delta(r_e \cos \gamma_e)} \frac{(65\,083\,000)}{(0.051)} (0.0001)$$

where 65 083 000 meters is the nominal entry range and 0.051° is the change in γ_e from its nominal value of -6.281° due to a change of 0.0001 in the cosine function.

The value of $(\sigma_{\gamma,e})_{\text{scatter}}$ was also checked at several times along the trajectory by simulated guidance corrections. For example, the perturbed trajectories in figure 9 were corrected by using the faired values of ΔV at $T_e = 9$ hours. Each trajectory was then propagated to the nominal entry altitude. The rms value of the entry-angle error was determined and was found to compare closely with that calculated by equation (4).

Effect of Maneuvering Error

The velocity-requirement ratio is also employed to determine the effect of guidance maneuvering error. Velocity-cutoff error comprises the major portion of this error. (See ref. 6.)

The rms entry-angle error due to velocity-cutoff error is shown in figure 23 for a typical 1σ value of 0.2 m/sec. This curve was determined by multiplying the reciprocal of the velocity-requirement ratio by 0.2 and corresponds to the case in which the guidance pointing angle λ is 90° , which is optimum for ΔV magnitude. It should be pointed out that by sacrificing the requirement for the ΔV magnitude, which is small – especially

in the case where midcourse guidance has been previously applied – and applying the ΔV vector at $\lambda = 0^\circ$, the effect of the maneuvering error can be reduced by about two-thirds. This same effect could be achieved by delaying the guidance maneuver. To obtain the two-thirds reduction, however, would require considerable delay (fig. 10), which may not be operationally feasible.

Combined Effect of Guidance Errors

The lowest plot in figure 23 shows the combined effect on entry-angle error due to measurement error, scatter error, and velocity-cutoff error according to the equation

$$\sigma_{\gamma,e} = \left[(\sigma_{\gamma,e})_{\text{meas}}^2 + (\sigma_{\gamma,e})_{\text{scatter}}^2 + (\sigma_{\gamma,e})_{\text{cutoff}}^2 \right]^{1/2}$$

With midcourse guidance.— Statistically speaking, the effect of measurement error has only a minor role in the overall guidance accuracy when a midcourse correction has been included; the velocity-cutoff error has the major effect. These facts are apparent when the curve for total $\sigma_{\gamma,e}$ is compared with the curves for these two effects shown in figures 22 and 23. It is significant to note that even if the instrument measurement error were doubled to 20 seconds of arc, the overall $\sigma_{\gamma,e}$ would be little affected. If the velocity-cutoff error were reduced in the manner previously described, the total $\sigma_{\gamma,e}$ would be negligible.

The data shown in figures 22 and 23 pertain to midcourse velocity errors, generally in the direction of the spacecraft velocity vector. An error analysis was performed for the situation where these errors were approximately normal to the velocity vector (fig. 8), and the results were found comparable with those shown for total $\sigma_{\gamma,e}$ in figure 23, providing $\theta_n = 90^\circ$. The main difference is that $\Delta\gamma_e/\Delta D$ more than doubles, and therefore the effect of measurement error increases.

Without midcourse guidance.— For the method without midcourse guidance comparison of the curve showing total effects and curves showing the three separate effects indicates that error in entry angle for this method is due chiefly to measurement error. If $\theta_n = 90^\circ$ at $T_e = 17.4$ hours, the total $\sigma_{\gamma,e}$ would be due mostly to scatter (fig. 17) and would be about the same as that shown in figure 23 where $\theta_n = 80^\circ$. If the curve in figure 21 representing no range measurement ($r_a \doteq r_n$) could be applied, the error in entry angle could be reduced for times earlier than $T_e = 12$ hours.

Maneuver time.— In regard to the total accuracy characteristics shown in figure 23 and for an entry corridor of $\pm 1^\circ$, it is apparent that with midcourse guidance, the approach guidance can be selected at any time along the trajectory because the 3σ value is always below 1° . For approach guidance without midcourse guidance, it appears from the errors

shown that an approach maneuver at about $T_e = 8$ hours or later would result in 3σ values of γ_e error below 1° . At $T_e = 8$ hours the average ΔV requirement is about 5 m/sec for the method without midcourse guidance and only about 0.5 m/sec for the method with midcourse guidance. The latter procedure, however, requires an additional average ΔV of about 3 m/sec for the midcourse maneuver under normal conditions.

CONCLUDING REMARKS

Results were obtained for simple onboard guidance of moon-to-earth trajectories which can be applied either with or without a midcourse correction. Normally one, but at most two, onboard angular measurements are required, from which a simple calculation yields the magnitude of the guidance velocity required to correct the trajectory. It was shown that the method which included the onboard midcourse correction is far superior. This method has much higher accuracy in controlling the entry angle and has more flexibility in the star selection. The method without midcourse guidance could be resorted to under the extreme condition that a midcourse correction were not available on the return trajectory.

Under certain conditions, a range measurement is not required; hence, the method could be applied to a procedure whereby the approach trajectory is controlled by earth-based line-of-sight measurements.

An error analysis showed that errors in the onboard guidance measurements do not primarily affect the overall approach-guidance accuracy if midcourse guidance has been included. Furthermore, the effect of guidance maneuvering error can be reduced by as much as two-thirds by changing the direction of the thrust vector or by delaying the guidance maneuver.

Langley Research Center,
National Aeronautics and Space Administration,
Hampton, Va., June 8, 1971.

APPENDIX A

SOME NOTES ON FIXED-TIME-OF-ARRIVAL ONBOARD MIDCOURSE GUIDANCE FOR TRANSEARTH TRAJECTORIES

One objective of the approach guidance procedure given in the main text of the report is to refine the effects of midcourse guidance error. Hence, the use of some type of midcourse guidance procedure was required as a prerequisite for the analysis of the approach procedure. The onboard method of reference 4 was employed for this analysis. In this reference, the procedure for calculating the midcourse maneuver velocity correction was developed from standard guidance equations, which make use of transition-matrix theory. The well-known fixed-time-of-arrival guidance, which guides the spacecraft to a given aim point on the nominal trajectory, was employed. Two basic equations which concern the navigator are

$$\overline{\Delta V}_F = [A] \begin{Bmatrix} D_I \\ D_{II} \\ D_{III} \end{Bmatrix}_{T,pf} + [B] \begin{Bmatrix} K_1 D_I \\ K_2 D_{II} \\ K_3 D_{III} \end{Bmatrix}_{T,pf}$$

$$\overline{\Delta V}_S = [C] \begin{Bmatrix} K_1 D_I \\ K_2 D_{II} \\ K_3 D_{III} \end{Bmatrix}_{T,pf}$$

The second midcourse correction $\overline{\Delta V}_S$ corrects the velocity error induced at the aim point by the derivation of the first midcourse velocity. The quantities A, B, and C are 3-by-3 matrices which are precomputed from nominal state-transition matrices and the direction cosines of three stars used for the measurements. The deviations D are the three position components as measured by the deviations of the perturbed trajectory from the nominal trajectory in the directions of the three stars. The constants K are predetermined from the variations shown in figure 24. The relation is

$$K = 1 + \frac{\delta D}{D}$$

The values in figure 24 were obtained from a sample of trajectories randomly perturbed at transearth injection. (See table I.) Figure 25 shows the geometry for the angles and

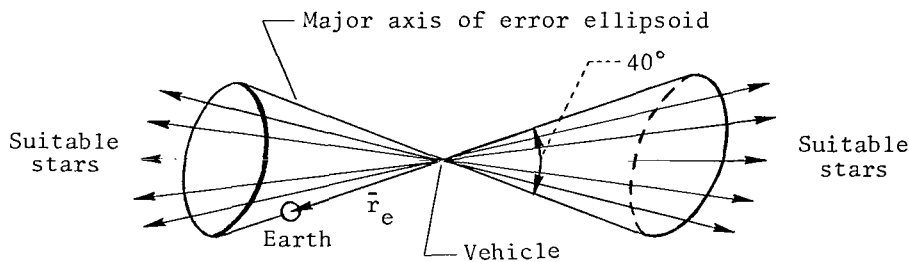
APPENDIX A - Continued

directions referred to in figure 24. The time $T_t = 9.5$ hours corresponds to the time of the position fix, and the time $T_t = 10$ hours is the time of the midcourse guidance maneuver.

Accuracy Characteristics

In reference 4 the method was thoroughly studied and found to be sufficiently accurate for midcourse control of translunar trajectories. Some results are presented herein which indicate that the method would apply as well, or better, to transearth trajectories.

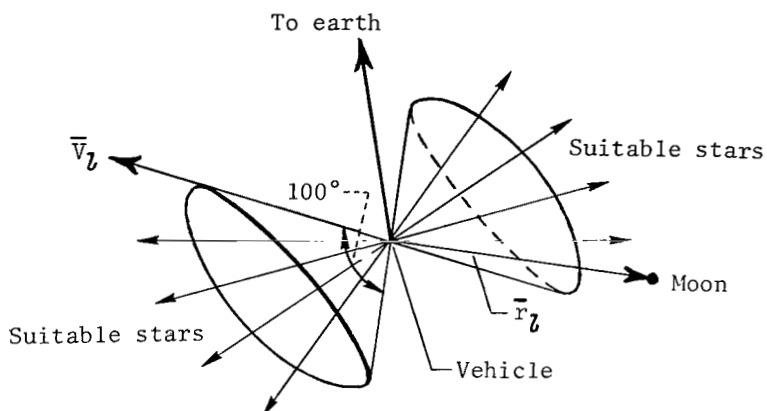
Effect of star selection. - One important characteristic of the method is the selection of the three measurement stars in directions such that δD can be accurately predicted from D calculated for the time of the position fix. This procedure eliminates the need for a second position fix and, hence, eliminates much of the effect of measurement error. For translunar trajectories, the region of acceptable stars for measurement is about 40° , as shown in sketch (a).



Sketch (a)

Figure 24 shows that for transearth trajectories, good prediction of δD may be obtained for an even larger region of stars. The only unacceptable direction is the bottom curve, characterized by large scatter and small sensitivity in D . Figure 25 and the upper five curves in figure 24 show that the acceptable region covers an angle greater than 90° in the selenocentric orbital plane as well as large out-of-plane angles. The region diagonally opposite this region would also be acceptable as may be seen in the sketch of the trajectory geometry (sketch (b)). (Values of δ near 90° provide no information on change in the orbital plane and should be avoided.)

APPENDIX A – Continued



Sketch (b)

Effect of transition-matrix theory.- The midcourse guidance method employs transition-matrix theory; therefore, another important characteristic of the method is the effect caused by the linear approximation made in using this theory. The state-transition matrix is strictly applicable only when the equations of vehicle motion are linear. Because of the actual nonlinearity of these equations, the midcourse guidance method is limited to perturbed trajectories that are reasonably close to the nominal trajectory. The data in table II show the results of correcting a sample of 33 transearth trajectories with the onboard midcourse method. No errors due to measurement error or in executing the guidance maneuver are included; the errors at the earth are due only to the effects of the linear approximation made in using the transition-matrix theory. As indicated by the large errors at the moon (at nominal perilune time), which could correspond to the transearth injection errors, the perturbed trajectories are widely dispersed about the nominal. The large dispersions are even more apparent at first midcourse guidance, which is about 20.5 hours beyond perilune time. Such large perturbations for injection out of lunar orbit are extremely improbable; however, these perturbations could possibly apply under emergency conditions when a translunar free-return trajectory is altered on approach to the moon to insure a 100-percent probability of miss.

The last two columns in table II indicate that widely dispersed trajectories can be reasonably controlled by guidance employing transition-matrix theory. It is interesting to note that the errors at the nominal entry altitude are smaller than those at the aim point. It is also seen that without the addition of the second midcourse velocity correction, the errors in spacecraft velocity and flight-path angle are small at the nominal entry altitude. These errors would not be reduced by including the second midcourse correction.

APPENDIX A – Concluded

Velocity Requirements

A comparison of midcourse-guidance velocity requirements of the onboard method for translunar and transearth trajectories is shown in table III. To establish the perturbed trajectories, injection errors of the same magnitude were applied at the earth and at the moon. These errors were applied by randomly changing components of the position by 10 km and components of the velocity by 10 m/sec. (See table I.) The velocity requirements pertain to a guidance maneuver time 10 hours from translunar or transearth injection. It can be noted in table III that the translunar requirements are 3 to 4 times higher than the transearth requirements. As expected, in both cases, the first midcourse velocity requirement is fairly insensitive to time selected for the aim point. However, the second midcourse velocity requirement does depend on the aim-point time, with the translunar (transearth) values decreasing (increasing) as the aim point is moved closer to the target body. The large transearth value for the aim point at nominal entry time is attributed to the relatively large magnitude of the spacecraft velocity at this point.

APPENDIX B

ESTIMATION OF ONBOARD MIDCOURSE VELOCITY ERROR

The magnitude of the guidance velocity error for onboard midcourse procedures can be estimated to a good degree of accuracy. The general form of the equation for onboard midcourse guidance, developed from reference 4, is

$$\overline{\Delta V}_F = [\phi_2]^{-1} \left\{ \overline{\Delta x}_{T, \text{pf}} \right\} - [\phi_2]^{-1} [\phi_1] \left\{ \overline{\Delta x}_{T, 1} \right\} + [\phi_2]^{-1} [\phi_1] \left\{ \overline{\Delta x}_{T, 1} \right\}$$

Since $[\phi_1]$ is essentially a unit matrix, then the following approximation can be made:

$$\overline{\Delta V}_F \approx [\phi_2]^{-1} \left\{ \overline{\Delta x}_{T, \text{pf}} - \overline{\Delta x}_{T, 1} \right\} + [\phi_2]^{-1} [\phi_1] \left\{ \overline{\Delta x}_{T, 1} \right\} \quad (\text{B1})$$

As shown in reference 4, error in the range measurement has the dominant effect on the error in $\overline{\Delta V}$. Also shown is the fact that for trajectories perturbed because of injection error, the position deviations $\overline{\Delta x}_{T, \text{pf}}$ and $\overline{\Delta x}_{T, 1}$ are essentially in the direction of the range vector. These conditions permit the $\overline{\Delta V}$ magnitude error to be determined by inserting appropriate errors for the position deviations in equation (B1). To accomplish this, a standard-deviation value of the range-measurement error can be determined for the time T_{pf} , based on instrument inaccuracies, and then substituted for $\overline{\Delta x}_{T, \text{pf}}$ as the error vector (in the range direction). The error vector $\overline{\Delta x}_{T, 1}$, which is somewhat larger in magnitude, can be determined from any perturbed trajectory by the percentage change in Δr from the times T_{pf} to T_1 .

APPENDIX C

VELOCITY REQUIREMENT FOR APPROACH GUIDANCE

An analytical expression for the variation of approach guidance velocity ΔV with the entry condition $r_e \cos \gamma_e$ is presented in this appendix. The velocity-requirement ratio $\Delta(\Delta V)/\Delta(r_e \cos \gamma_e)$ is useful for error analysis. The equation which follows is the exact expression for this ratio (at small values of ΔV) and was determined by differentiating equation (1) with respect to $r_e \cos \gamma_e$. Except for distances very close to the earth, only the middle term of the equation is significant. For example, at $T_e = 9$ hours ($r \approx 110\,000$ km) the first and last terms contribute only about 1 percent to the total value.

$$\begin{aligned} \frac{\partial(\Delta V)}{\partial(E)} = & \frac{2r^2VE \cos(\gamma + \lambda) [\cos \gamma + \cos \lambda \cos(\gamma + \lambda)]}{[r^2 \cos^2(\gamma + \lambda) - E^2]^2} \\ & \pm \frac{[r^2 \cos^2(\gamma + \lambda) + E^2] \left\{ (r^2 - E^2) V^2 \sin^2 \lambda + [r^2 \cos^2(\gamma + \lambda) - E^2] \left(\frac{2\mu}{r_e} - \frac{2\mu}{r} \right) \right\}^{1/2}}{[r^2 \cos^2(\gamma + \lambda) - E^2]^2} \\ & \mp \frac{E^2 \left(V^2 \sin^2 \lambda + \frac{2\mu}{r_e} - \frac{2\mu}{r} \right)}{[r^2 \cos^2(\gamma + \lambda) - E^2] \left\{ (r^2 - E^2) V^2 \sin^2 \lambda + [r^2 \cos^2(\gamma + \lambda) - E^2] \left(\frac{2\mu}{r_e} - \frac{2\mu}{r} \right) \right\}^{1/2}} \end{aligned}$$

where

$$E = r_e \cos \gamma_e$$

REFERENCES

1. Havill, C. Dewey: An Emergency Midcourse Navigation Procedure for a Space Vehicle Returning From the Moon. NASA TN D-1765, 1963.
2. McLean, John D.; and Cicolani, Luigi S.: Midcourse Guidance for Return From the Moon to a Geographically Fixed Landing Site. NASA TN D-3318, 1966.
3. Hamer, Harold A.: A Concept of Midcourse and Terminal Guidance With Single Position Fixes Obtained From Onboard Optical Measurements. Proceedings of the ION National Space Meeting on Space Navigation - Present and Future, Inst. of Navigation, Apr. 1969, pp. 31-55.
4. Hamer, Harold A.; Johnson, Katherine G.; and Blackshear, W. Thomas: Midcourse-Guidance Procedure With Single Position Fix Obtained From Onboard Optical Measurements. NASA TN D-4246, 1967.
5. Warner, M. R.; Nead, M. W.; and Hudson, R. H.: The Orbit Determination Program of the Jet Propulsion Laboratory. Tech. Mem. No. 33-168 (Contract NAS 7-100), Jet Propulsion Lab., California Inst. Technol., Mar. 18, 1964.
6. Hamer, Harold A.; and Johnson, Katherine G.: An Approach-Guidance Method Using a Single Onboard Optical Measurement. NASA TN D-5963, 1970.

TABLE I.- TRANSLUNAR AND TRANSEARTH PERTURBATIONS USED
TO DETERMINE MIDCOURSE GUIDANCE CHARACTERISTICS

Case	Injection-position perturbation, km			Injection-velocity perturbation, m/sec		
	Δx	Δy	Δz	$\Delta \dot{x}$	$\Delta \dot{y}$	$\Delta \dot{z}$
1	-10					
2		-10				
3			10			
4				10		
5					10	
6						10
7	-10			-10		
8	10			10		
9		-10				-10
10		10				10
11			-10	10		
12			10	-10		
13			-10		10	
14			10		-10	
15		-10		10		
16		10		-10		
17		10		10		
18			10		10	
19			10	10		
20	10			-10		

TABLE II. - THE 1σ RESULTS FOR WIDELY DISPERSED
 TRANSEARTH TRAJECTORIES BEFORE AND AFTER
 "PERFECT" MIDCOURSE GUIDANCE CORRECTION

Quantity	Before correction		After correction	
	At nominal perilune time (transearth injection)	At first midcourse guidance	At aim point (nominal entry time)	At nominal entry altitude
s, km	896	3323	284	65.3
u, m/sec	208	41.8	^a 243	
Δr_l , km	125	1558		
Δr , km			36.4	
δV_l , m/sec	27.7	17.1		
δV , m/sec			^a 39.8	^b 1.33
$\Delta \gamma_e$, deg				^b 0.29
Δt , sec				28.8

^a ΔV_S included.

^b ΔV_S not included.

TABLE III.- VELOCITY REQUIREMENTS FOR
 FIXED-TIME-OF-ARRIVAL GUIDANCE
 $[\Delta V_F \text{ at 10 hours from injection}]$

Location of aim point	Average values	
	ΔV_F , m/sec	$\Delta V_S/\Delta V_F$
Translunar trajectories		
Lunar sphere of influence ($T_p \approx 14.6$ hr)	55	0.13
Nominal perilune time	54	0.08
Transearth trajectories		
$T_e = 17$ hr	15.7	0.17
$T_e = 9$ hr	15.2	0.16
$T_e = 1$ hr	14.7	0.27
Nominal entry time	14.7	3.98

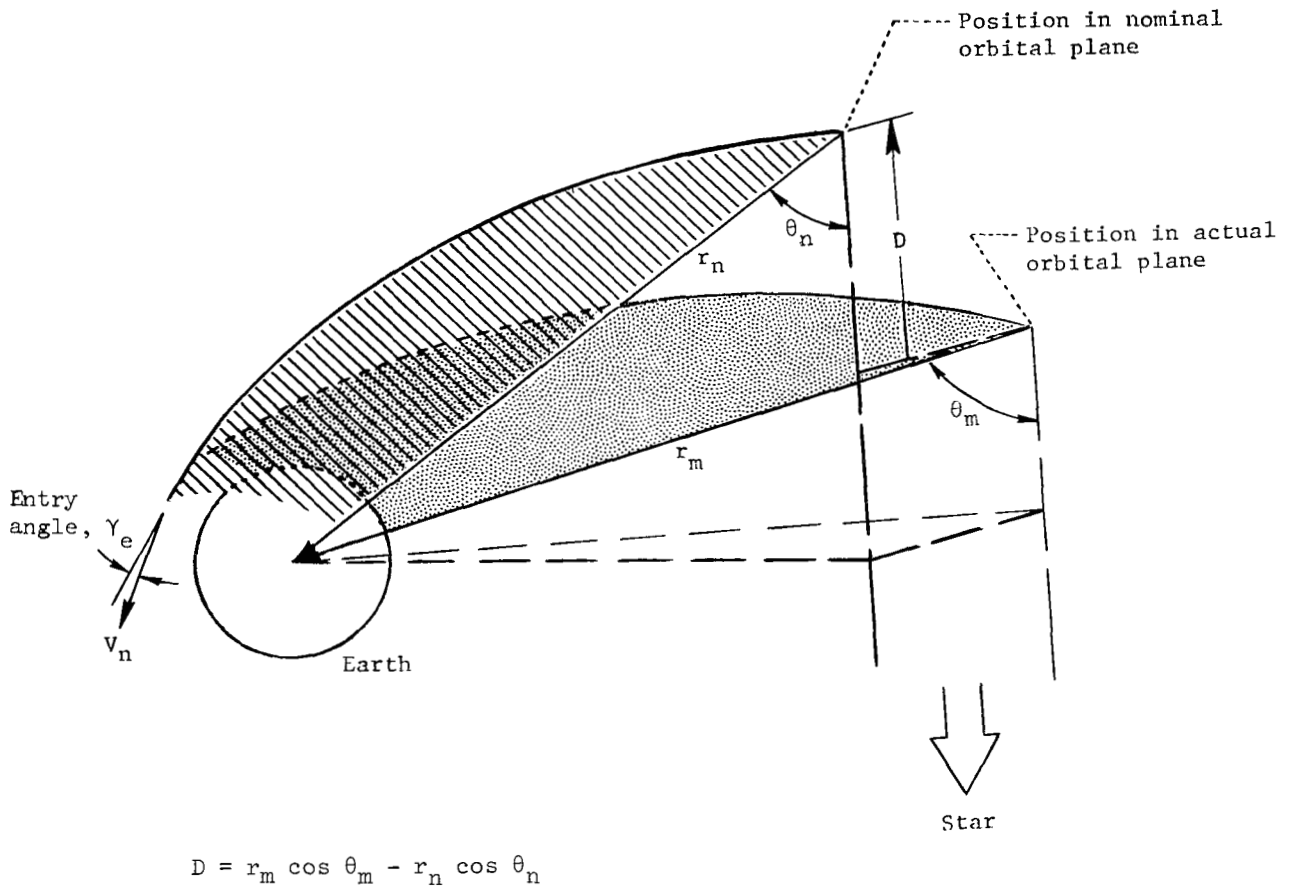


Figure 1.- Sketch showing approach guidance geometry.

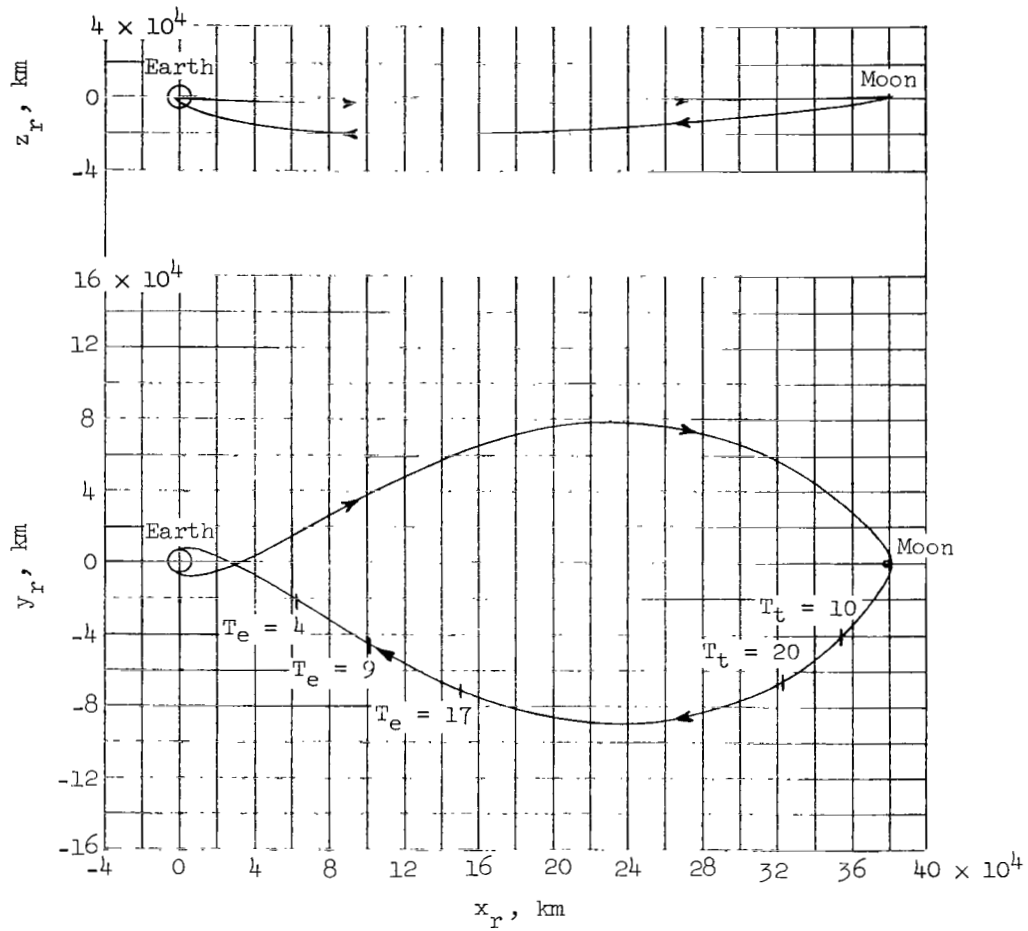
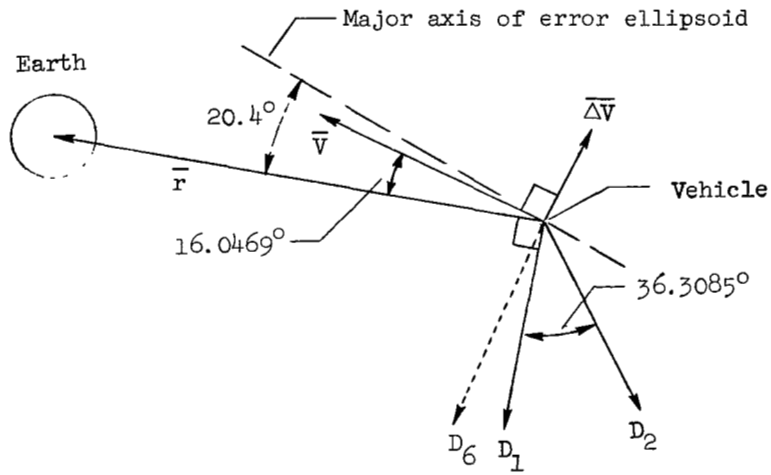
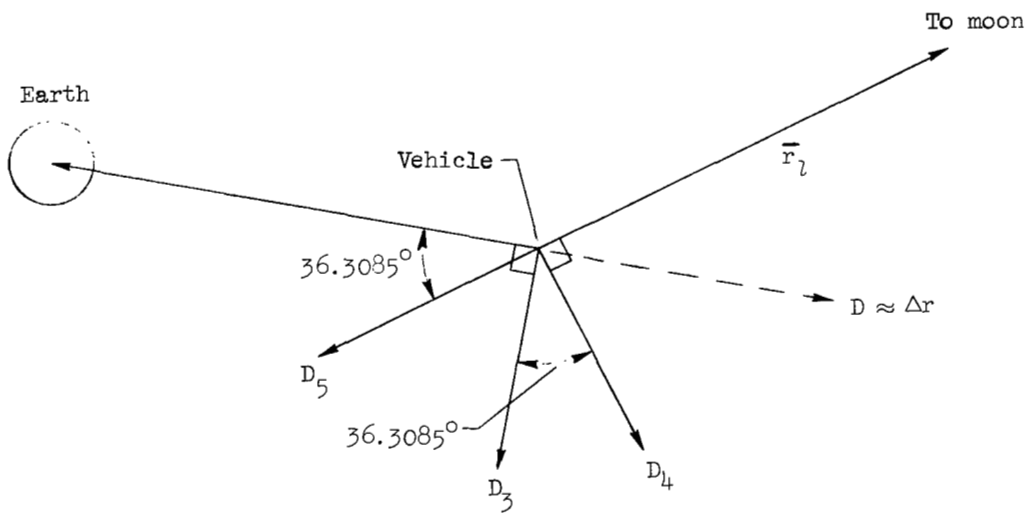


Figure 2.- Nominal trajectory. (T_t is hours from perilune; T_e is hours to entry.)

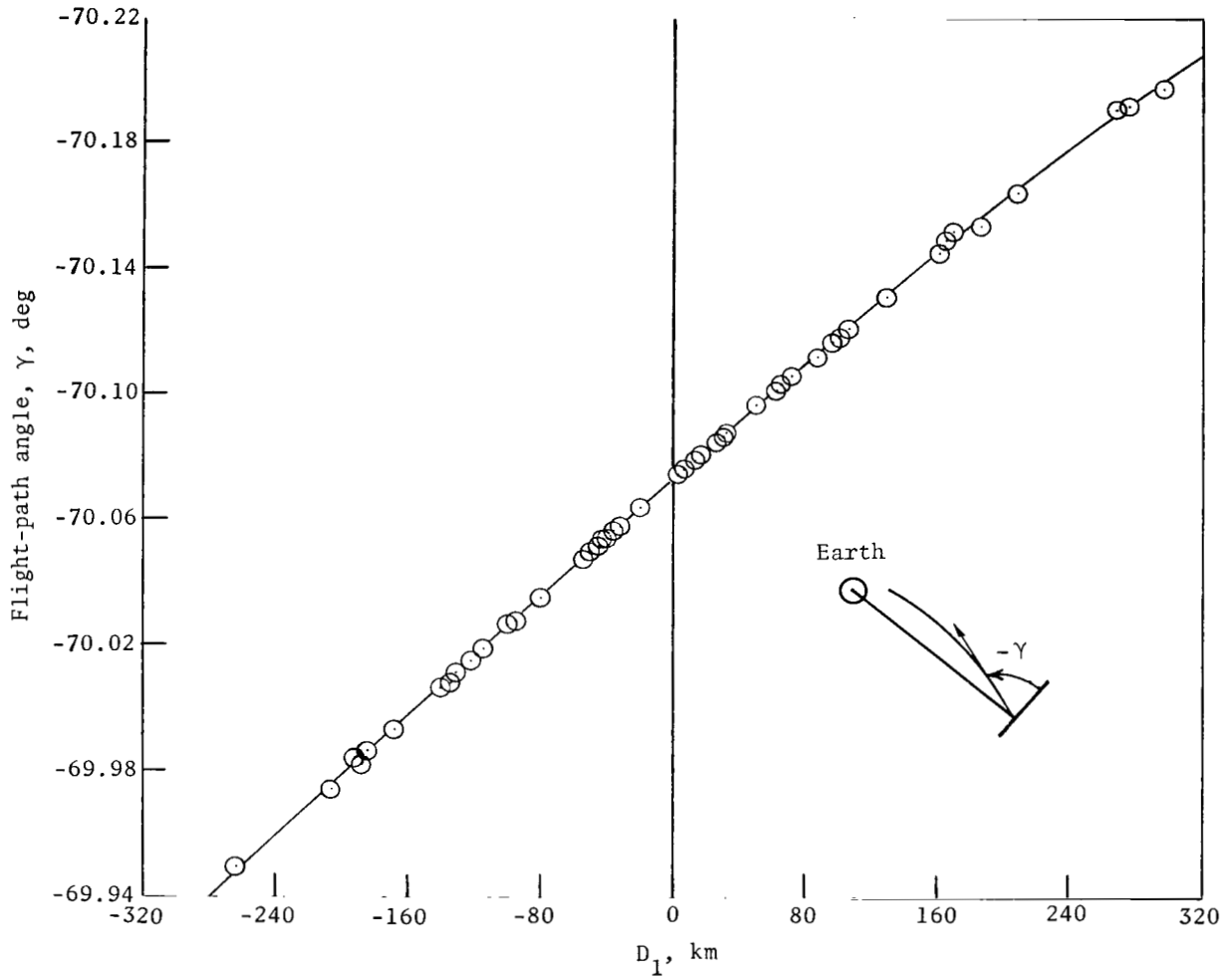


(a) Nominal orbital plane.



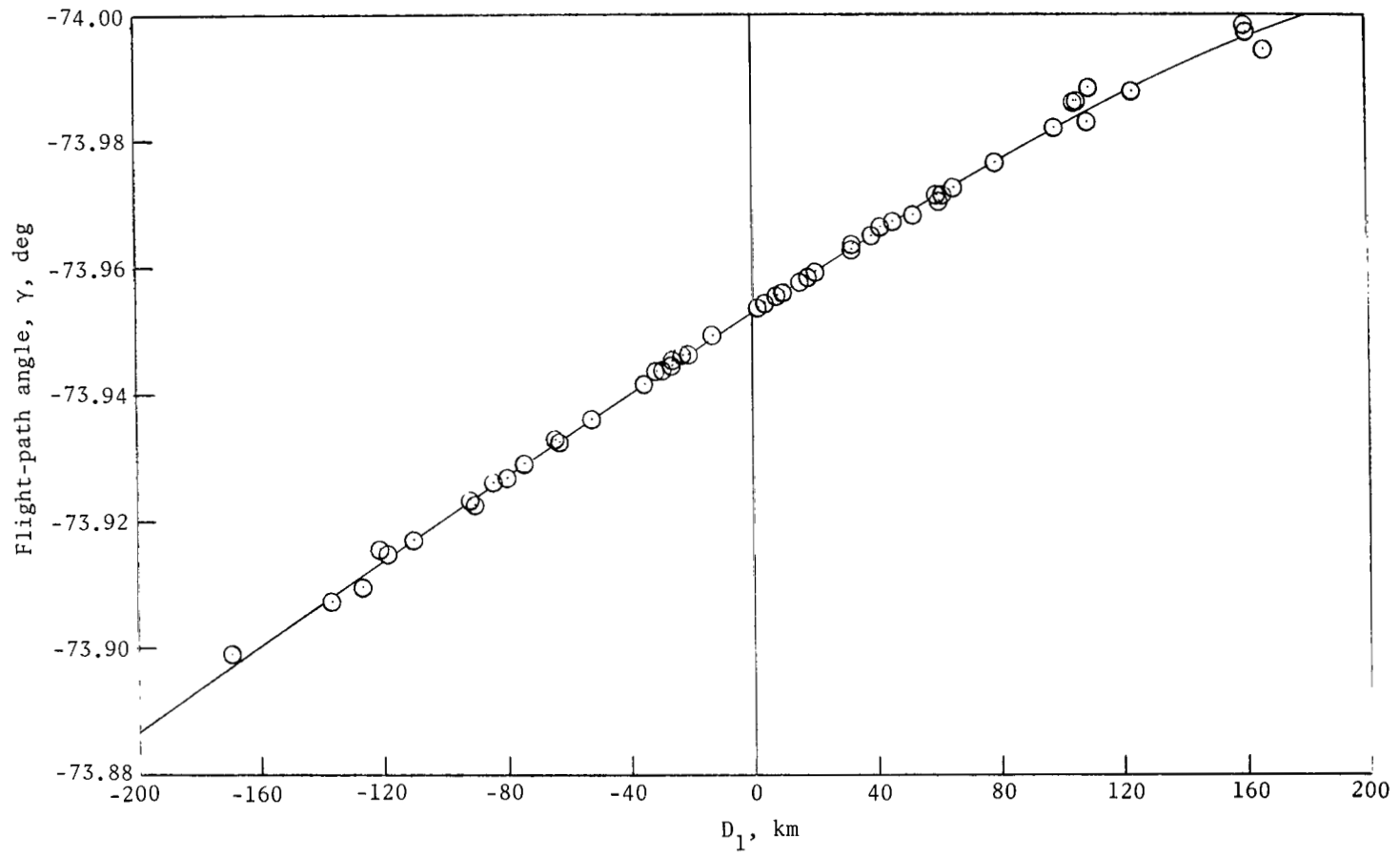
(b) Nominal instantaneous earth-moon-vehicle plane.

Figure 3.- Illustration showing direction of deviations studied for $T_e = 9$ hours.



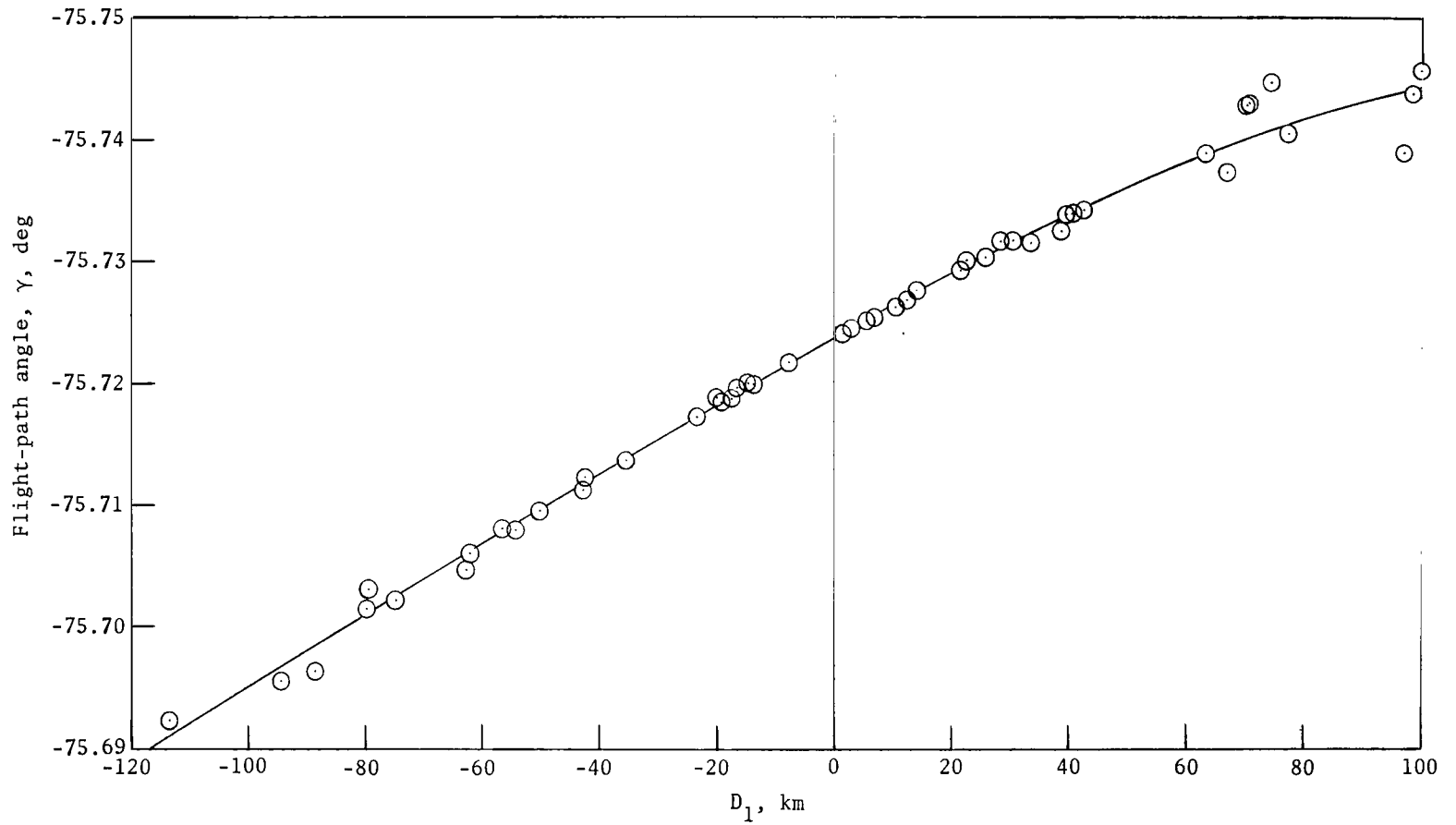
(a) $T_e = 4$ hours.

Figure 4.- Flight-path angle correlation with deviation. Deviation D_1 is in nominal orbital plane with $\theta_n = 90^\circ$.



(b) $T_e = 9$ hours.

Figure 4.- Continued.



(c) $T_e = 17$ hours.

Figure 4.- Concluded.

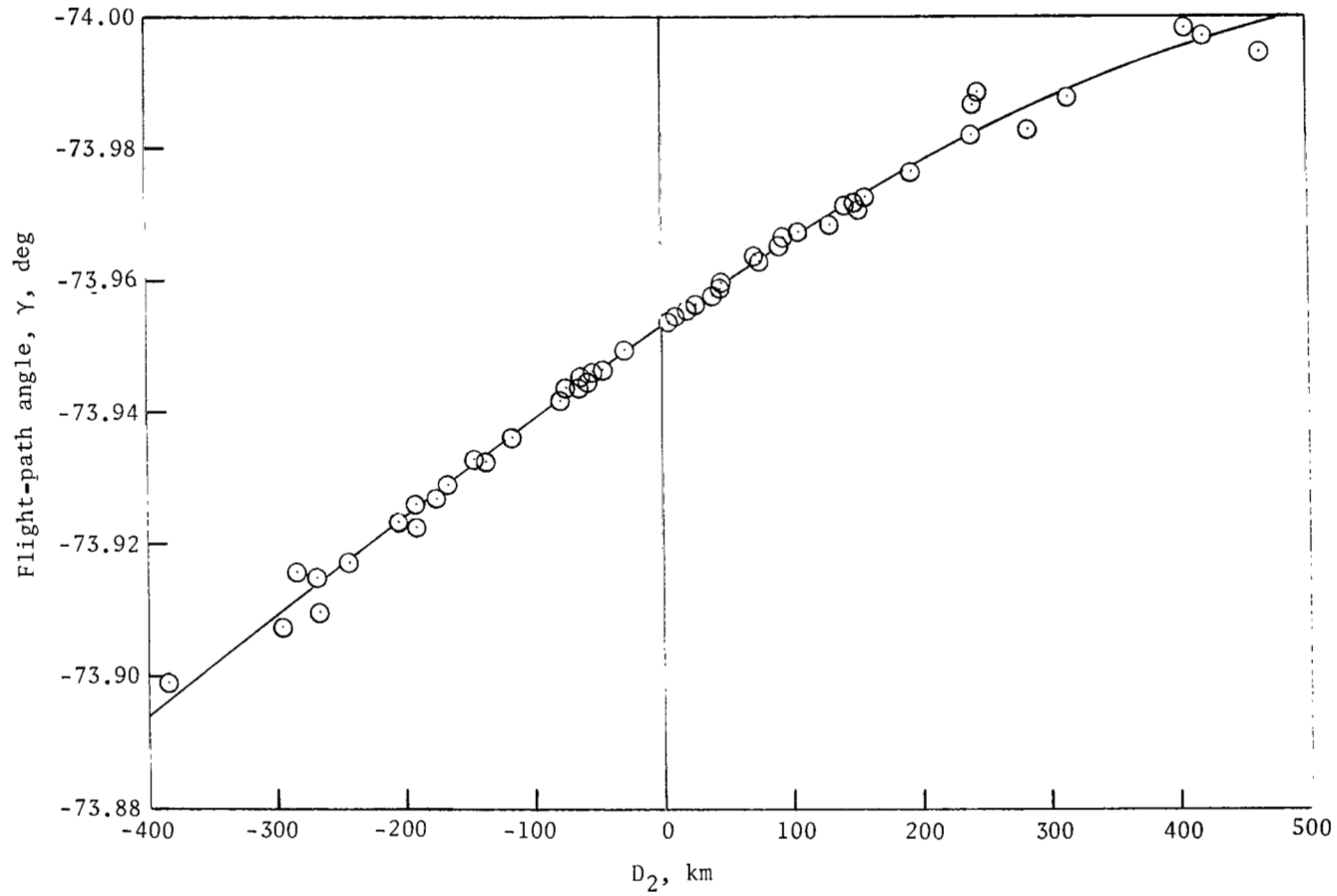


Figure 5.- Flight-path angle correlation with deviation at $T_e = 9$ hours.
Deviation D_2 is in nominal orbital plane with $\theta_n = 126.3085^\circ$.

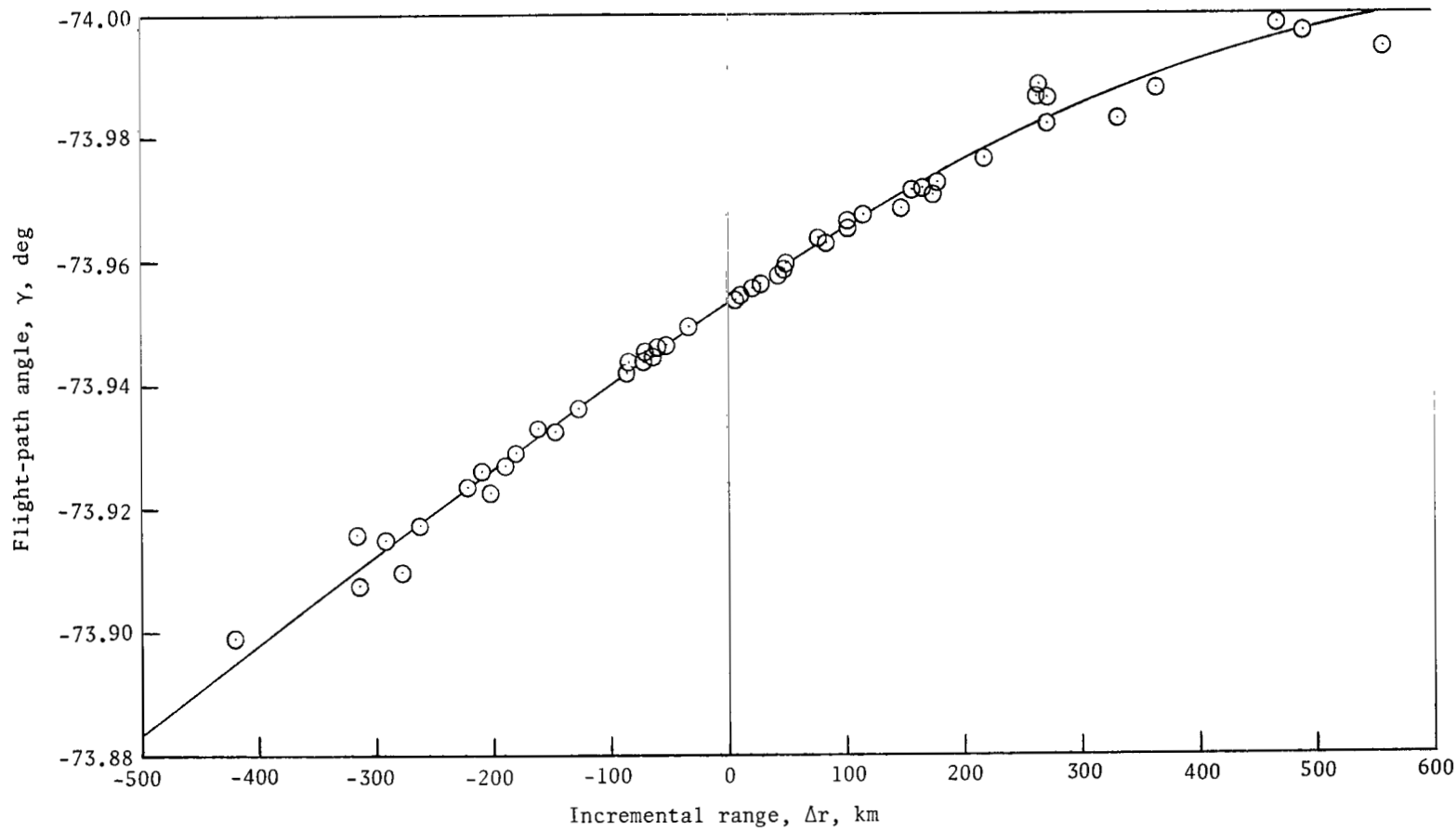
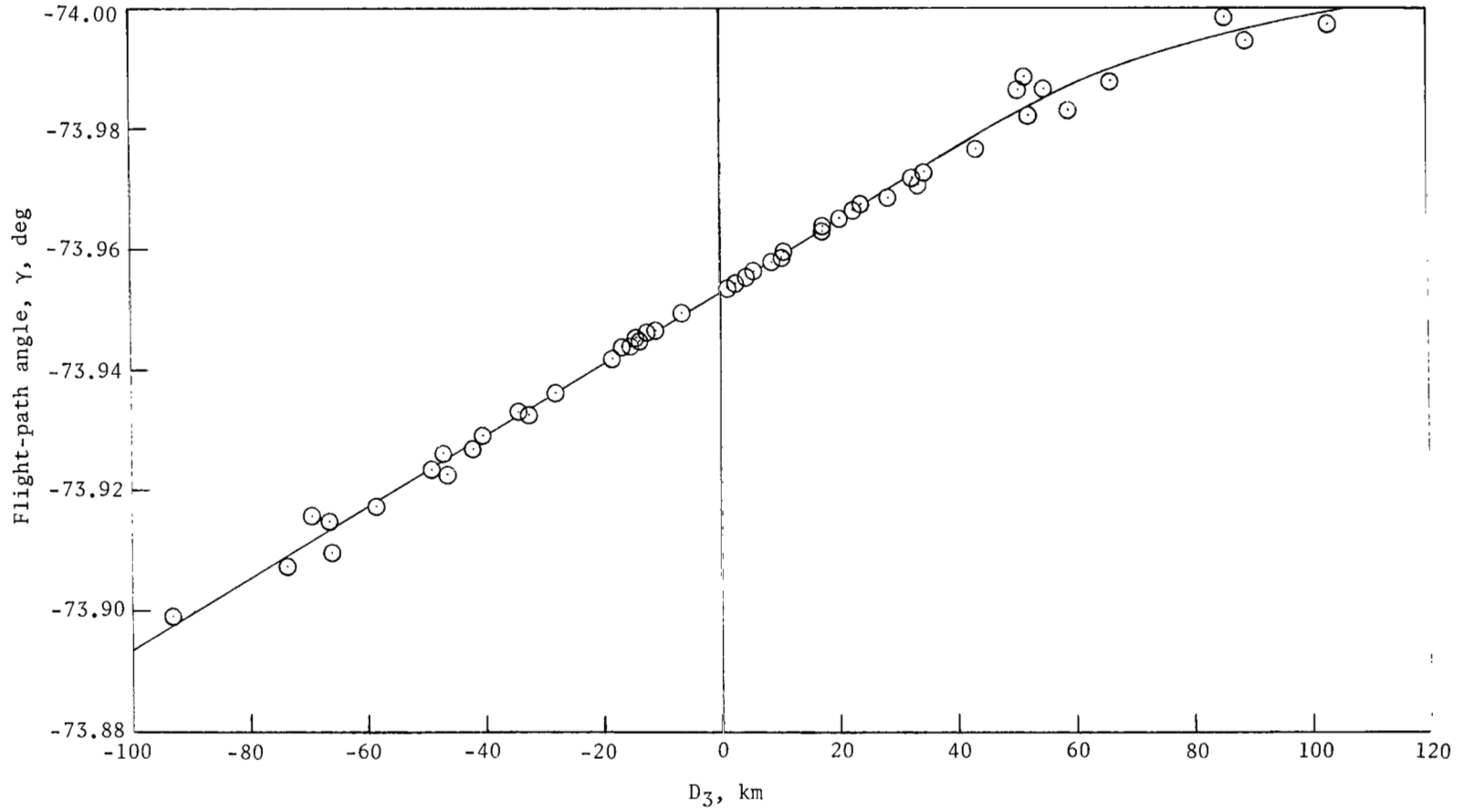
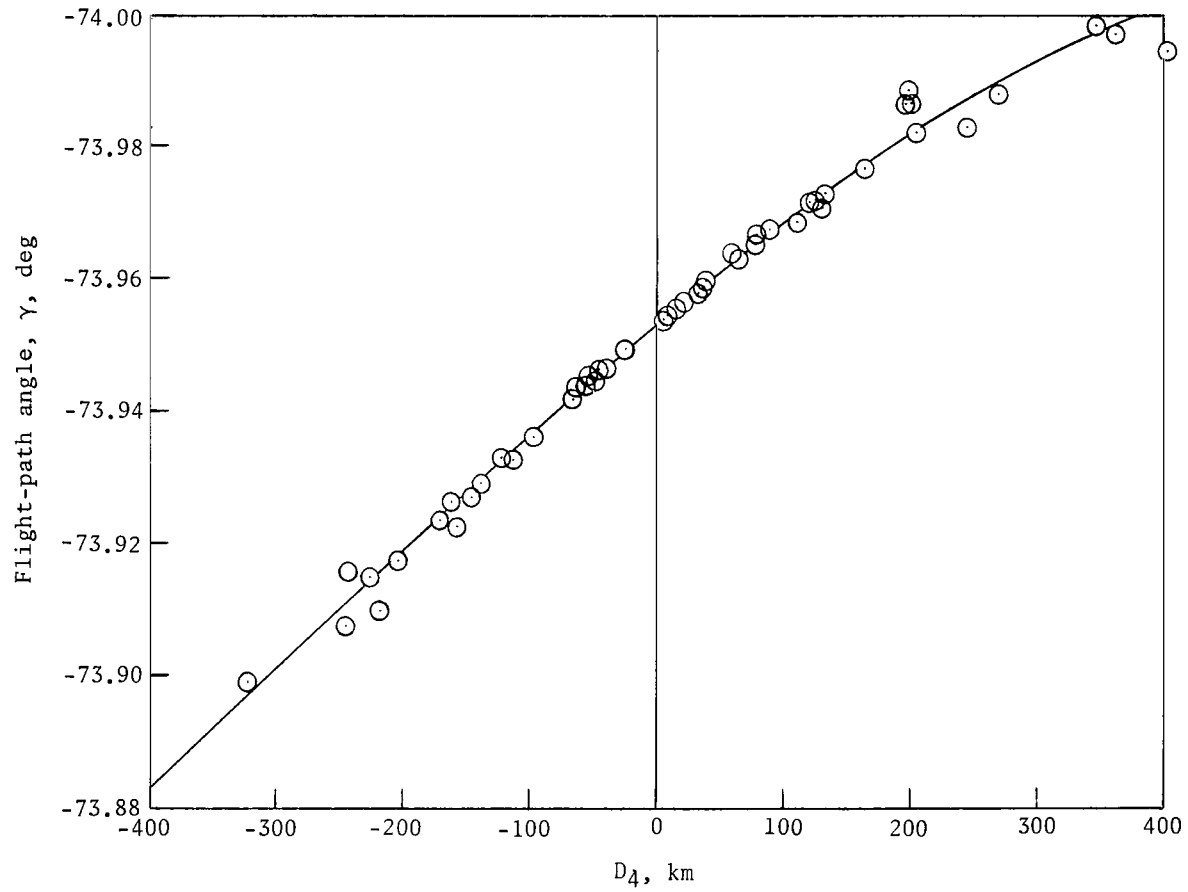


Figure 6.- Flight-path angle correlation with incremental range at $T_e = 9$ hours and $r_n = 110\ 310$ km.



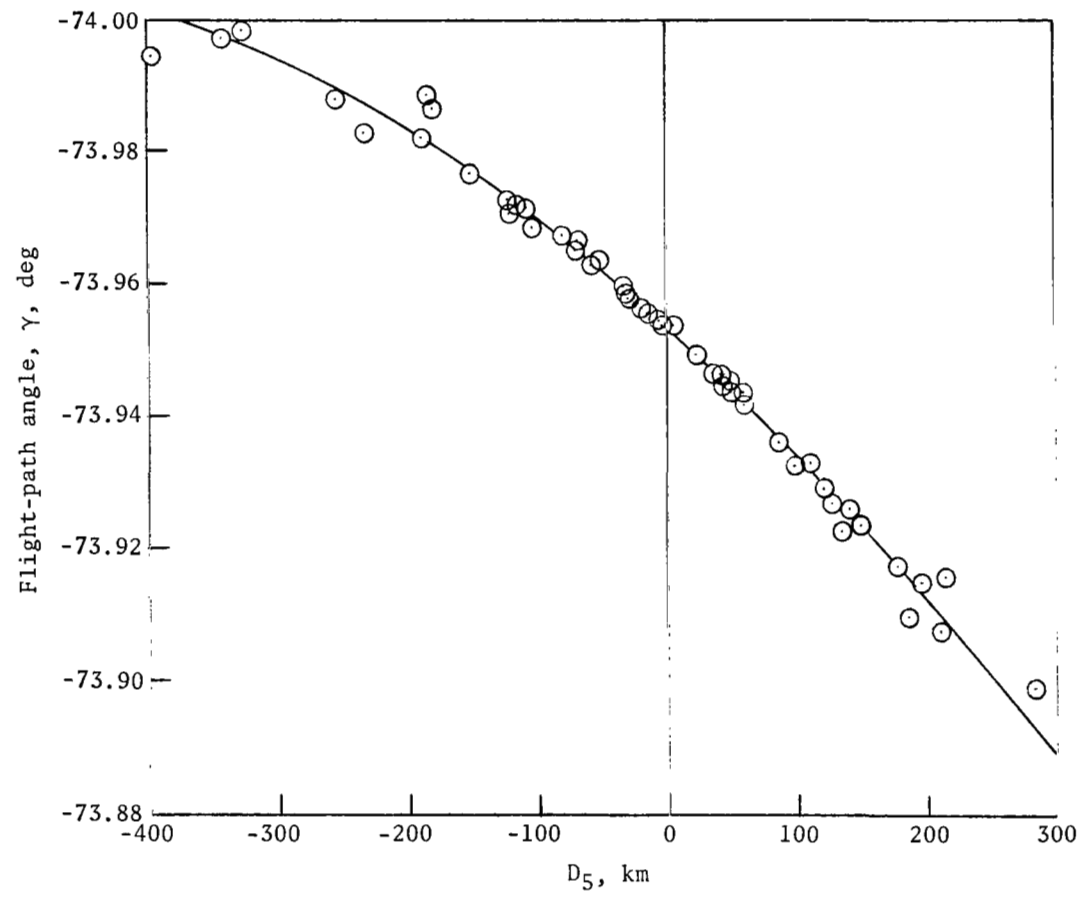
(a) Deviation perpendicular to nominal geocentric range vector.

Figure 7.- Flight-path angle correlation with deviations taken in instantaneous earth-moon-vehicle plane at $T_e = 9$ hours.



(b) Deviation perpendicular to nominal selenocentric range vector.

Figure 7.- Continued.



(c) Deviation parallel to nominal selenocentric range vector.

Figure 7.- Concluded.

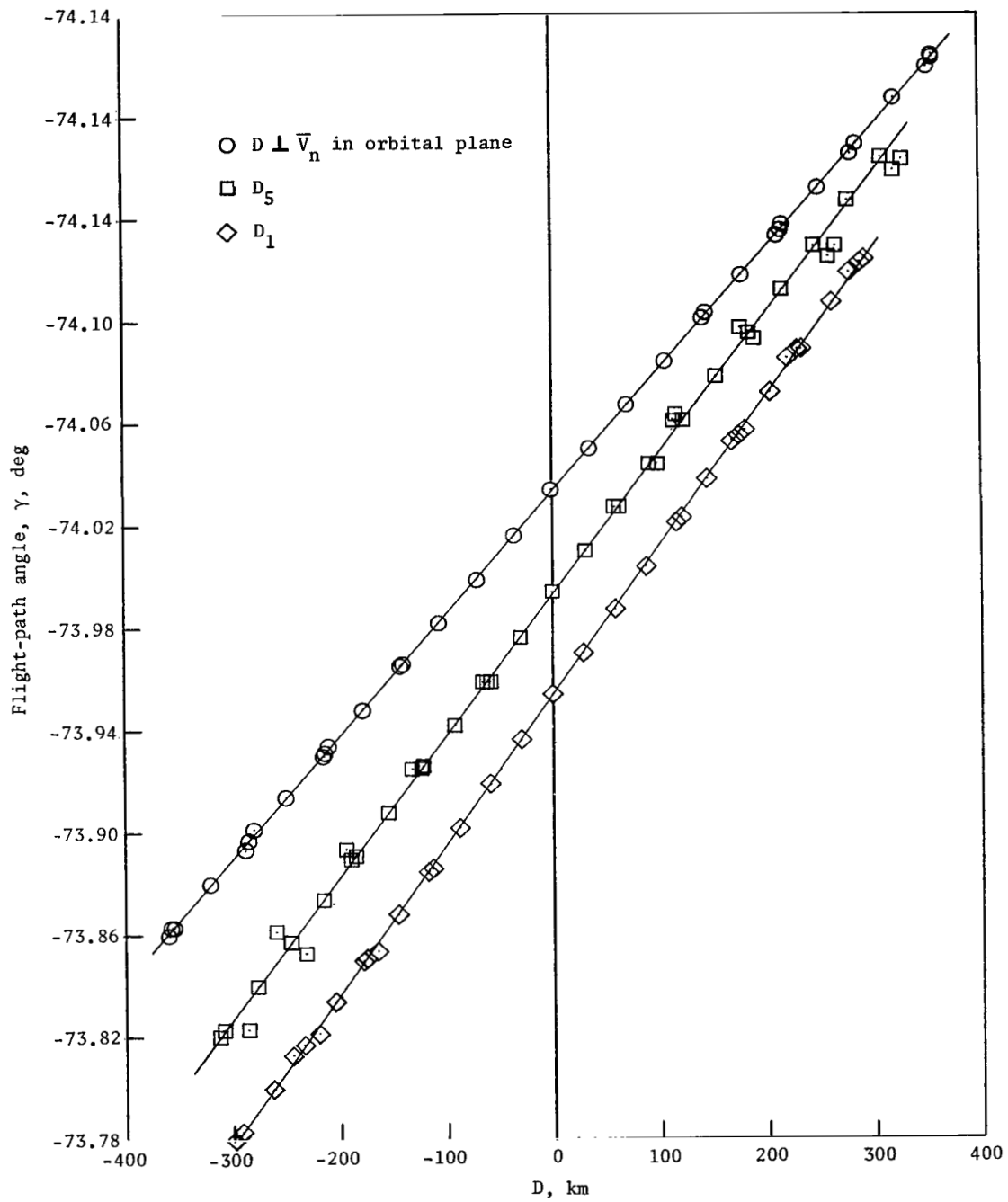


Figure 8.- Flight-path angle correlation with deviations taken at $T_e = 9$ hours. Midcourse guidance velocity errors are approximately normal to spacecraft velocity vector. (Note staggered scale.)

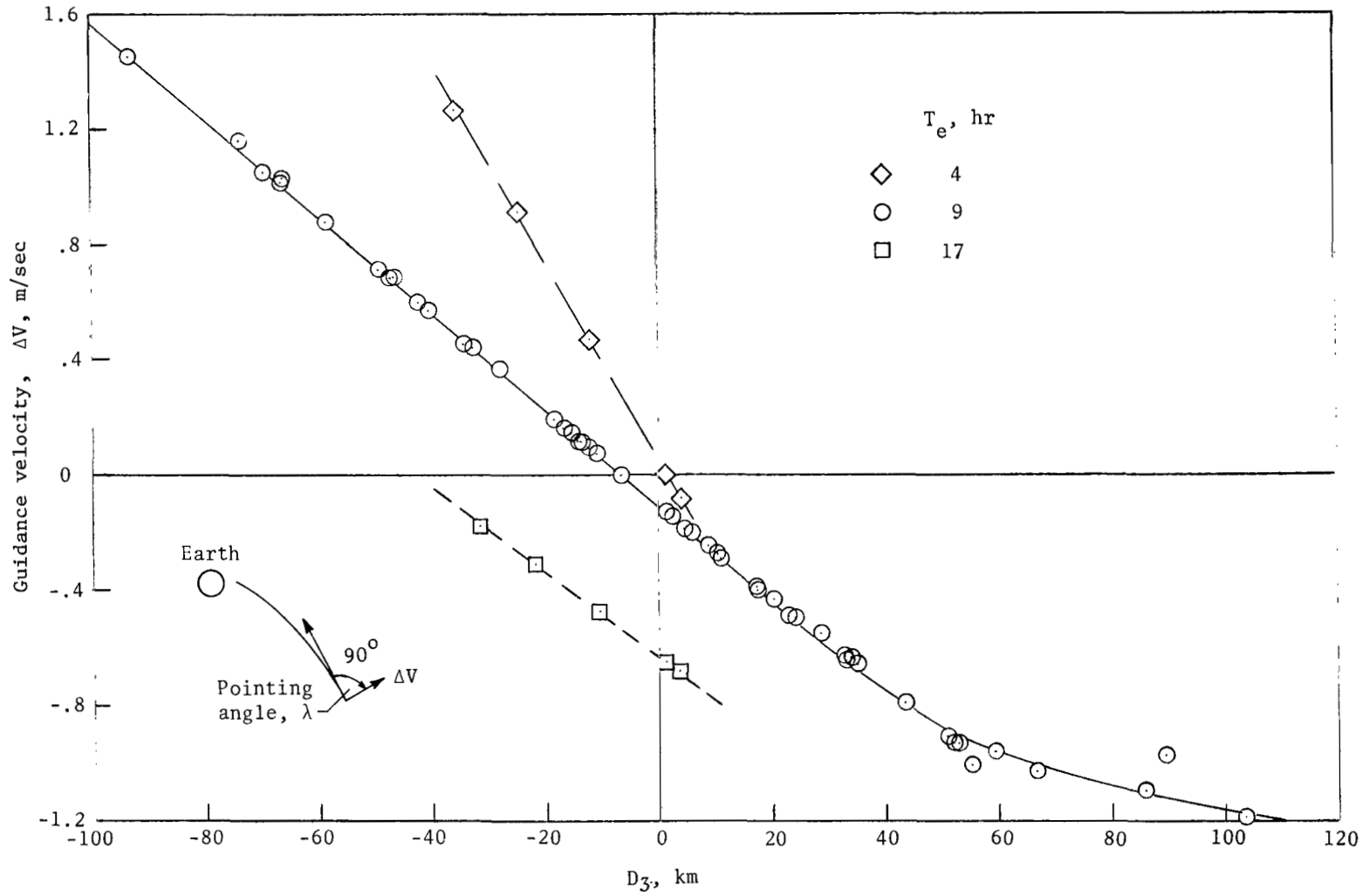


Figure 9.- Correlation of approach guidance velocity with deviation D_3 .

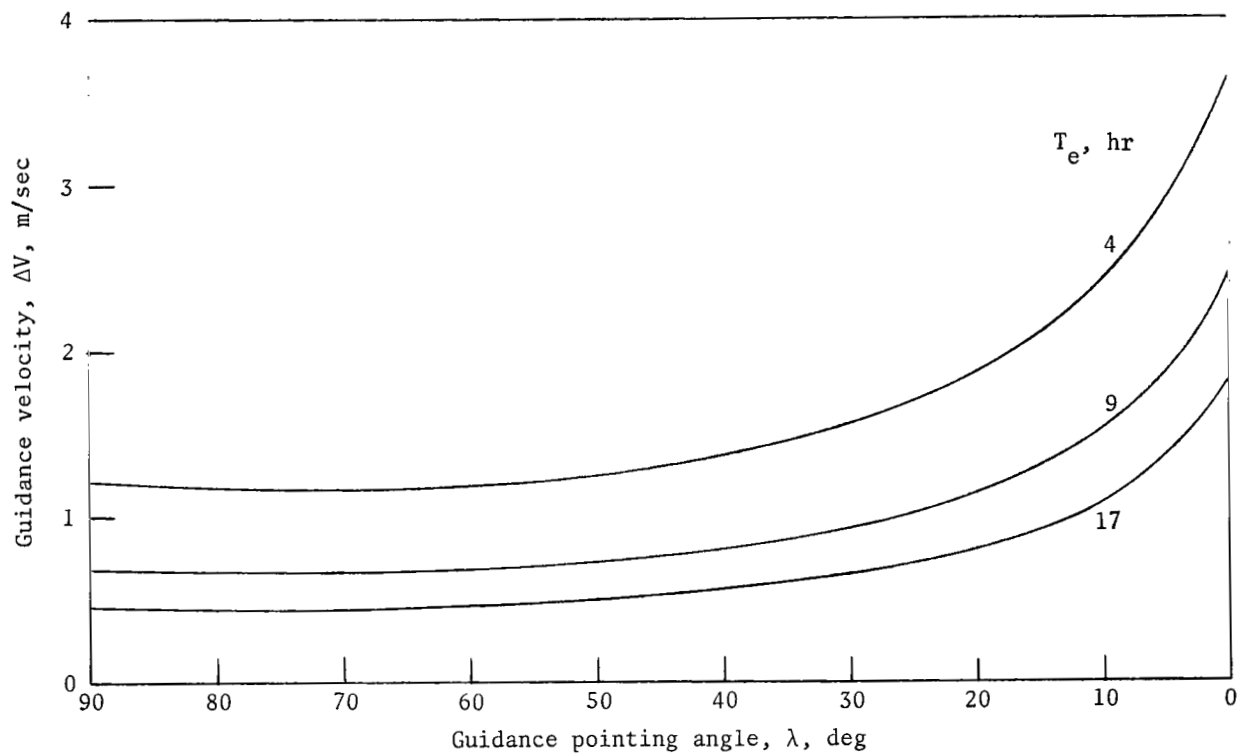


Figure 10.- Example of approach guidance velocity required for a typical perturbed trajectory.

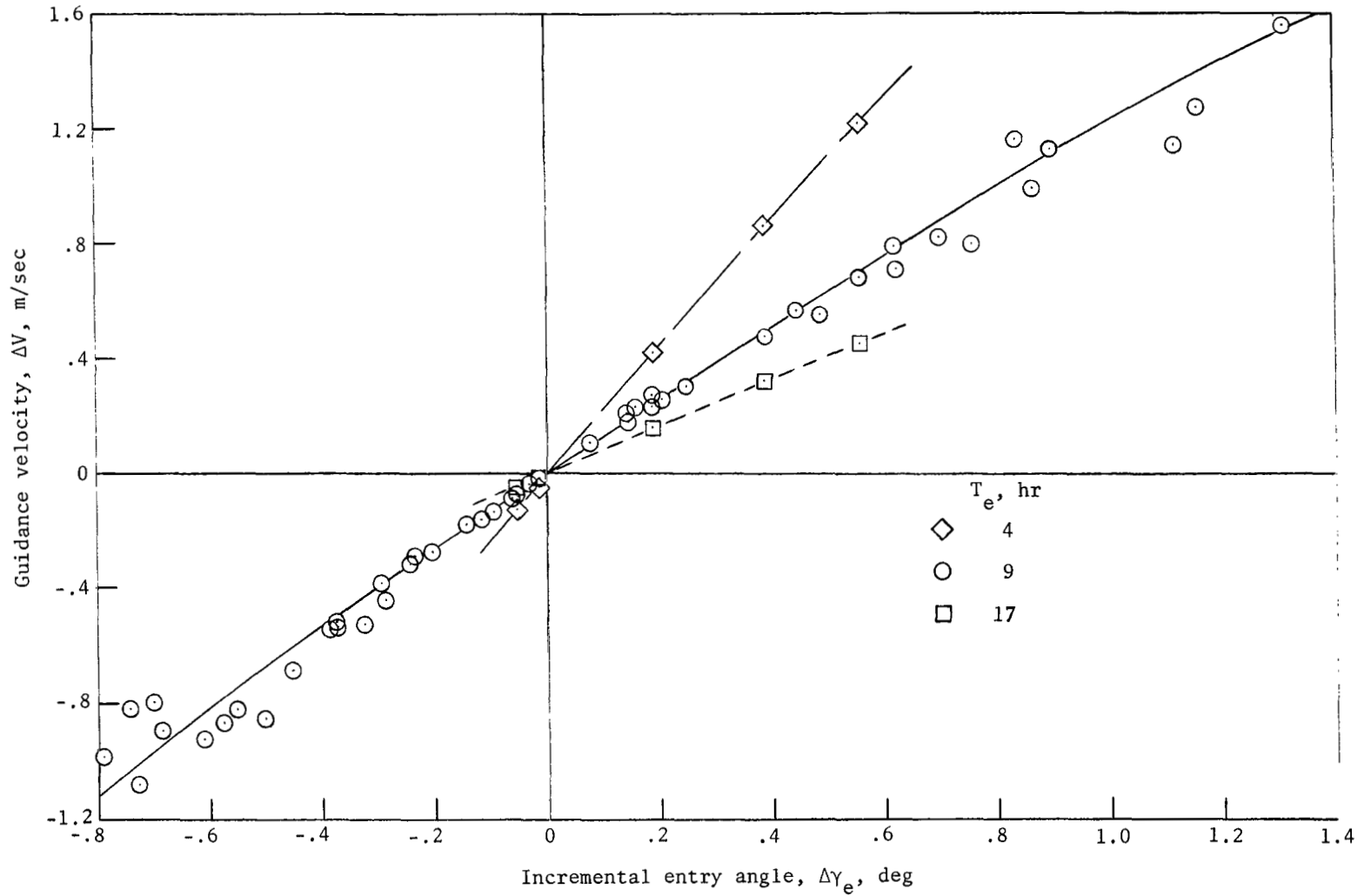


Figure 11.- Approach guidance velocity requirement as a function of incremental entry angle at nominal entry altitude. $\lambda = \pm 90^\circ$.

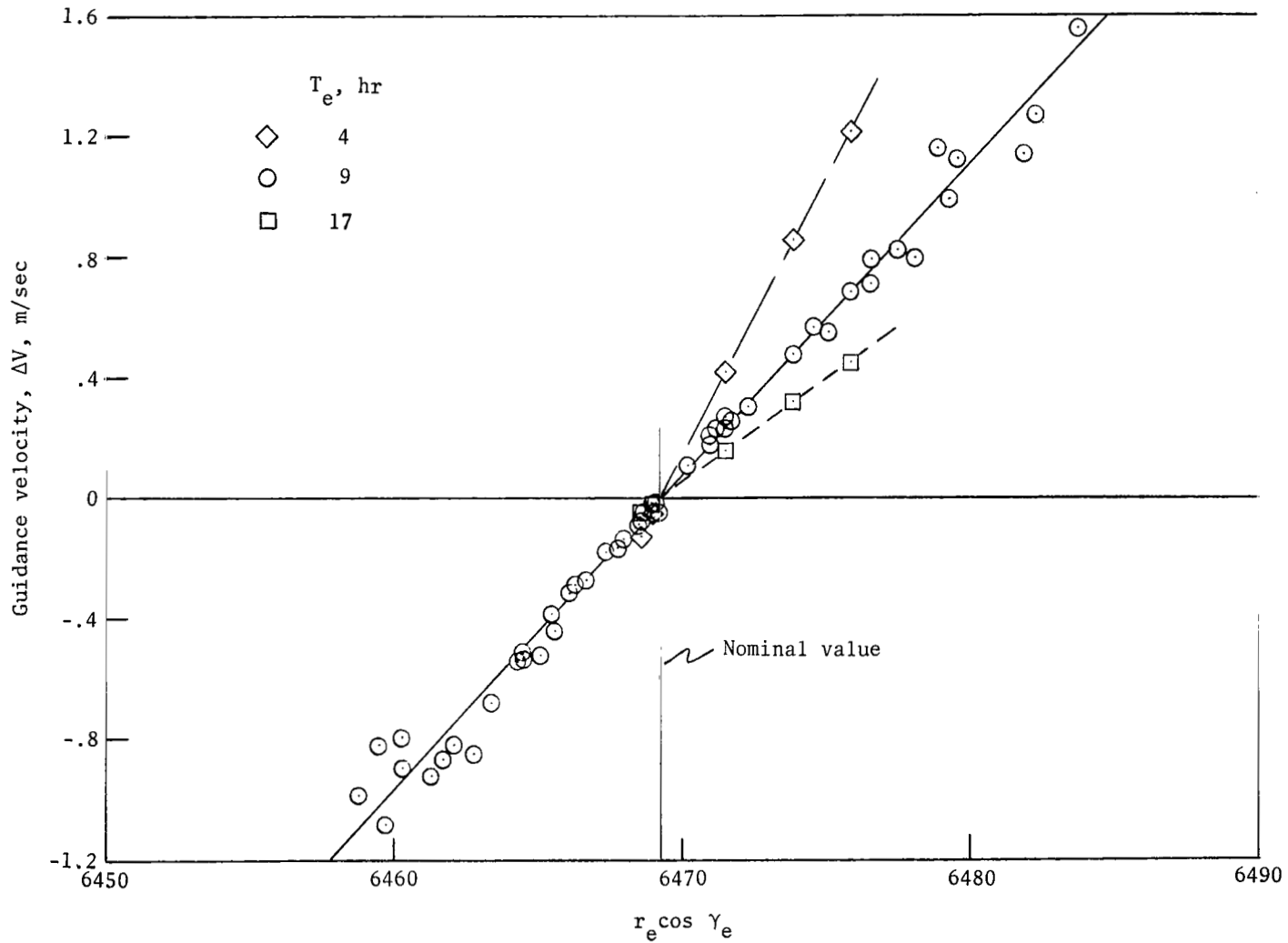


Figure 12.- Approach guidance velocity requirement as a function of product of nominal entry range and cosine of entry angle. $\lambda = \pm 90^\circ$.

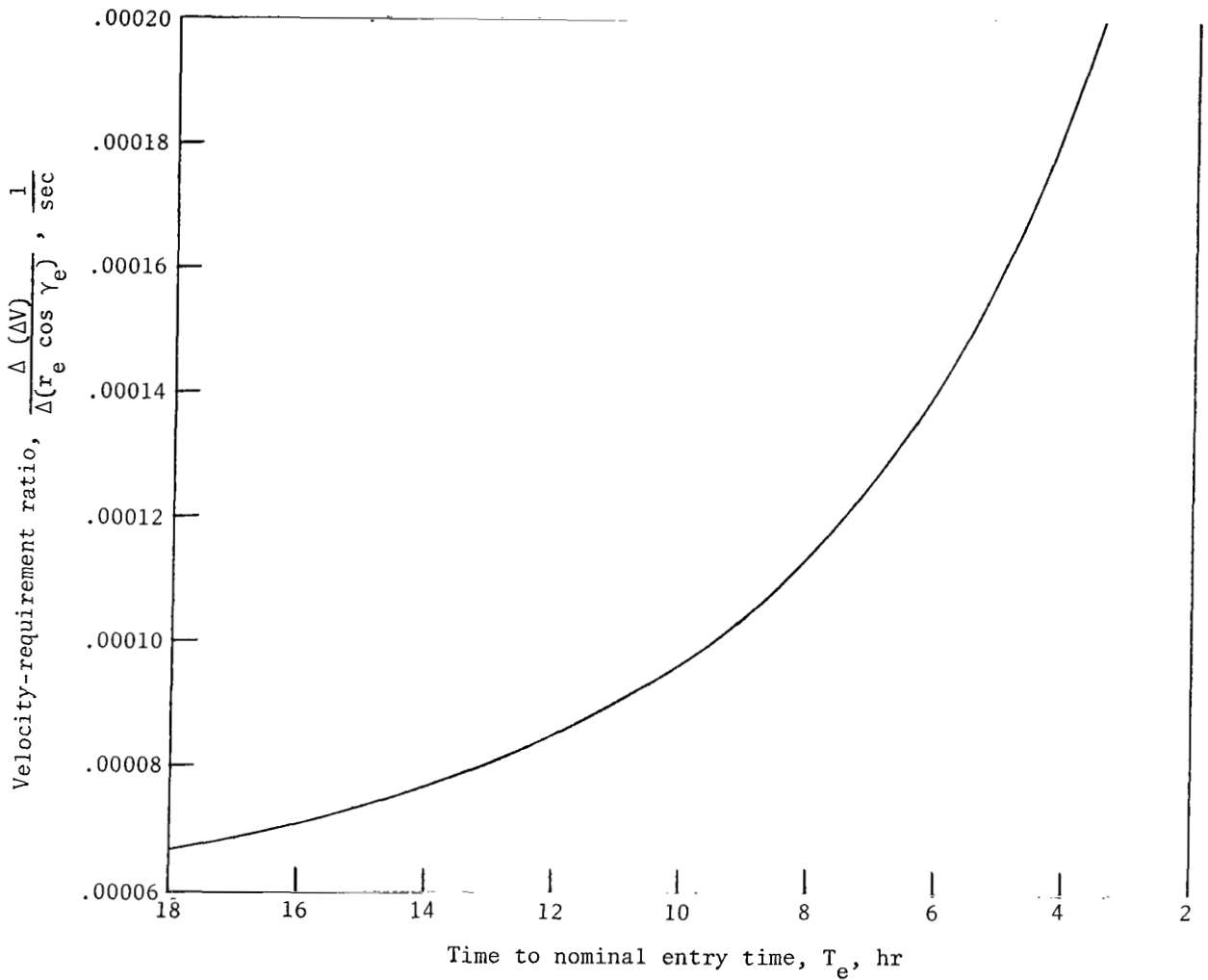


Figure 13.- Guidance-velocity-requirement ratio as a function of time to entry. $\lambda = \pm 90^\circ$.

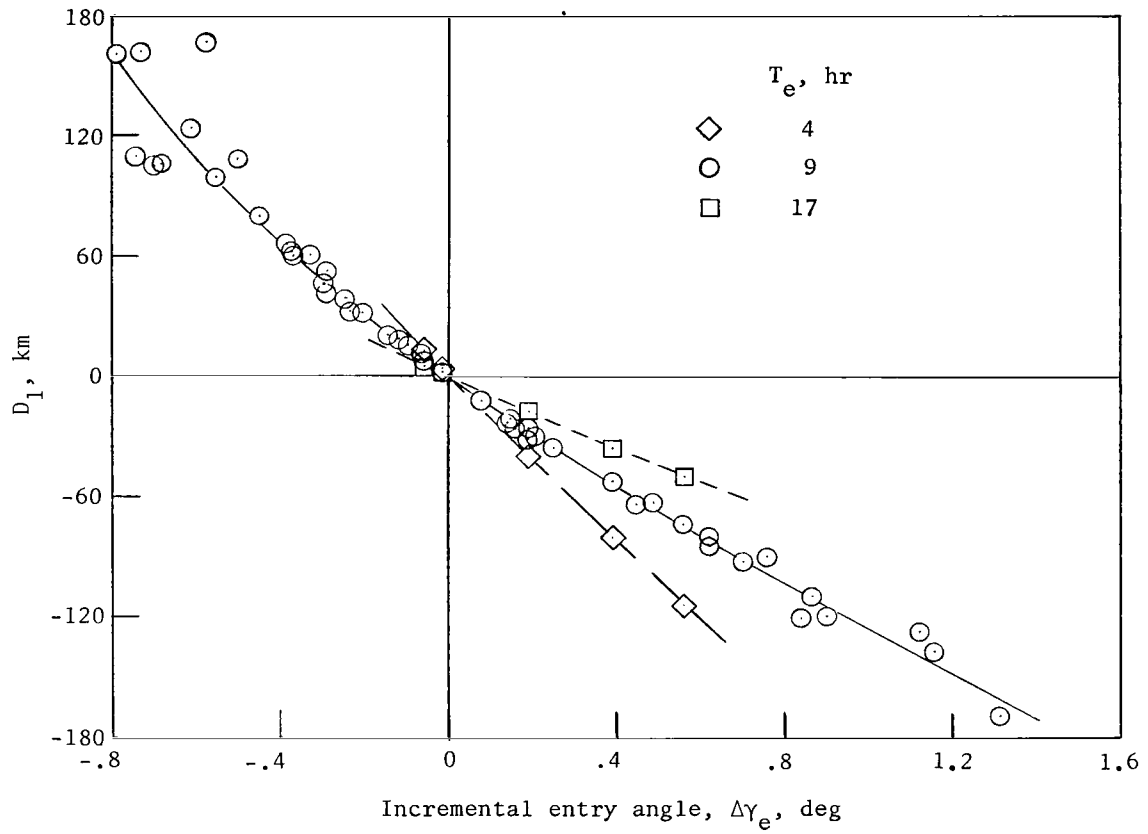


Figure 14.- Sensitivity of entry angle at nominal entry altitude with deviation D_1 .

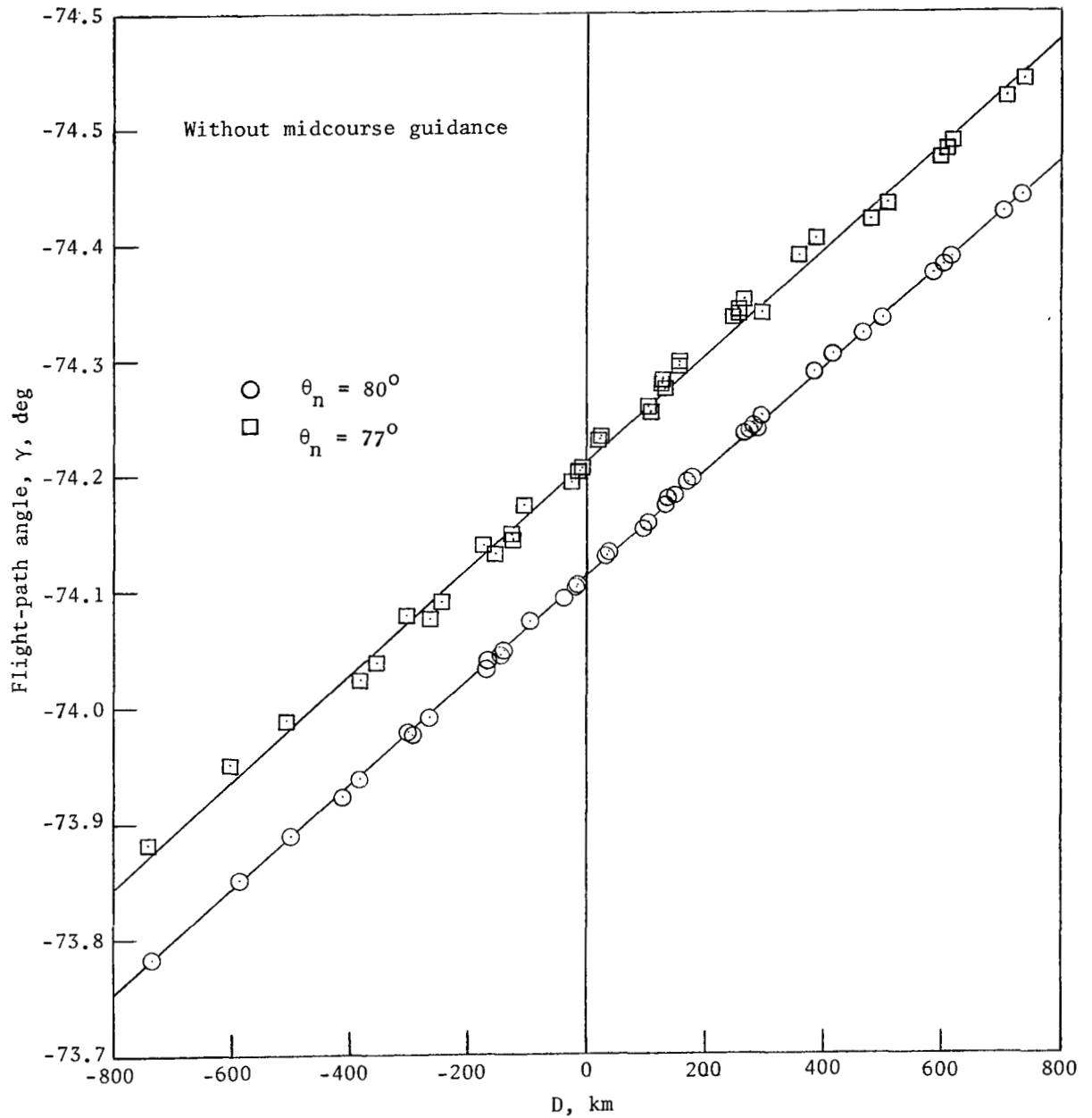
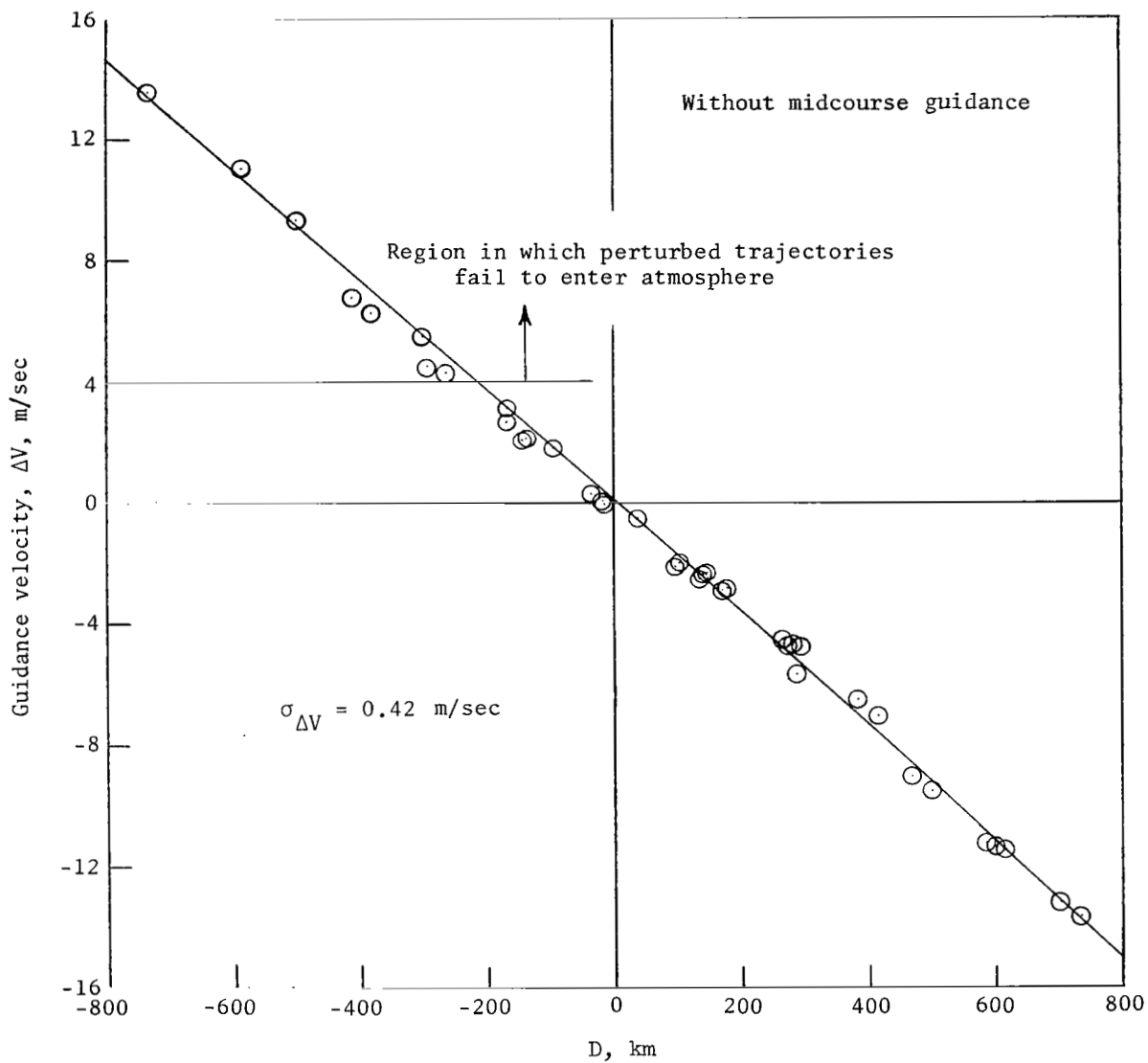
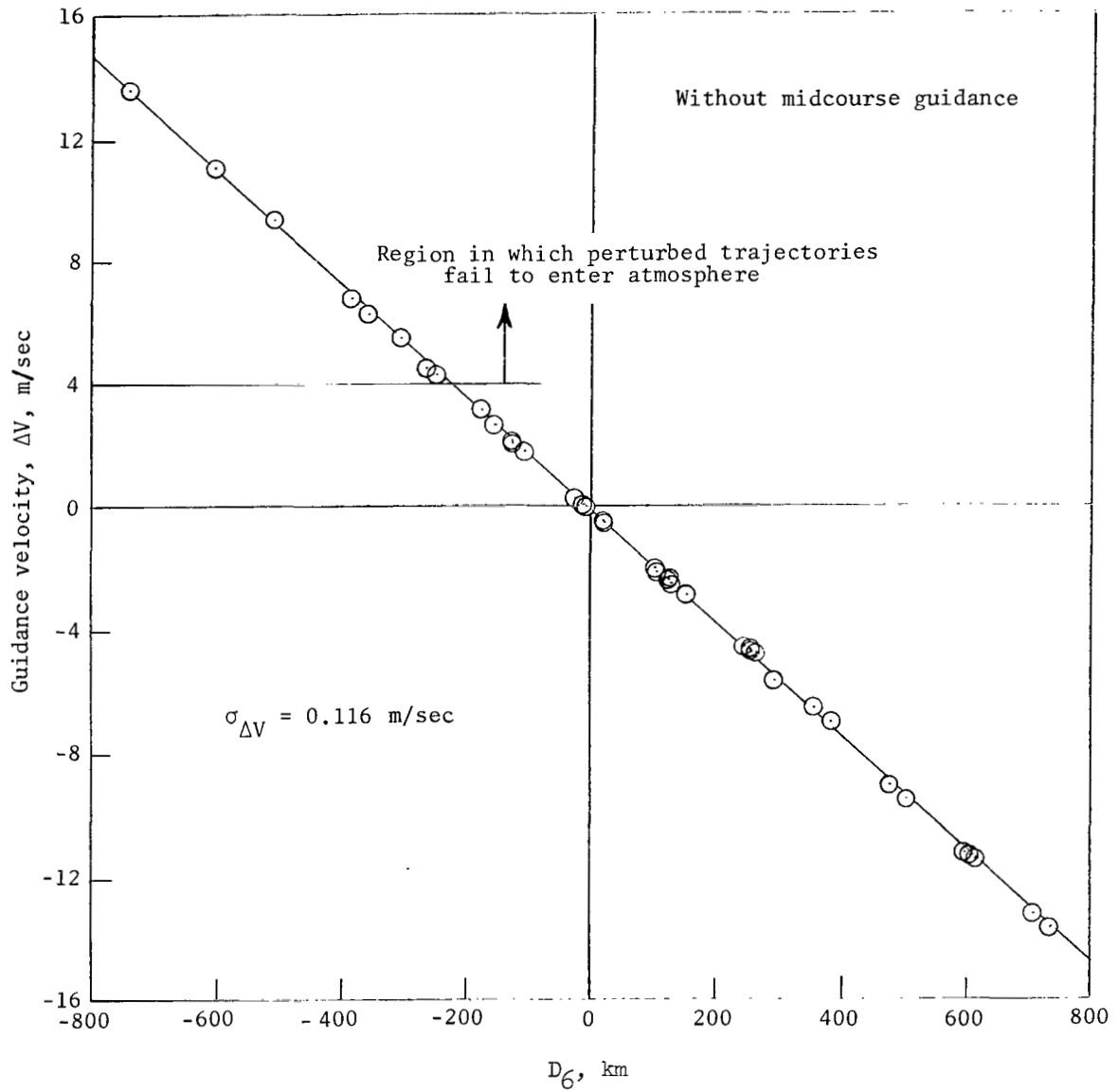


Figure 15.- Correlation of flight-path angle with deviation at $T_e = 9.4$ hours. Deviation D is in nominal orbital plane. (Note staggered vertical scale.)



(a) $\theta_n = 80^\circ$.

Figure 16.- Correlation of approach guidance velocity with deviation at $T_e = 9.4$ hours.
 $\lambda = \pm 90^\circ$; D is in nominal orbital plane.



(b) $\theta_n = 77^\circ$.

Figure 16.- Concluded.

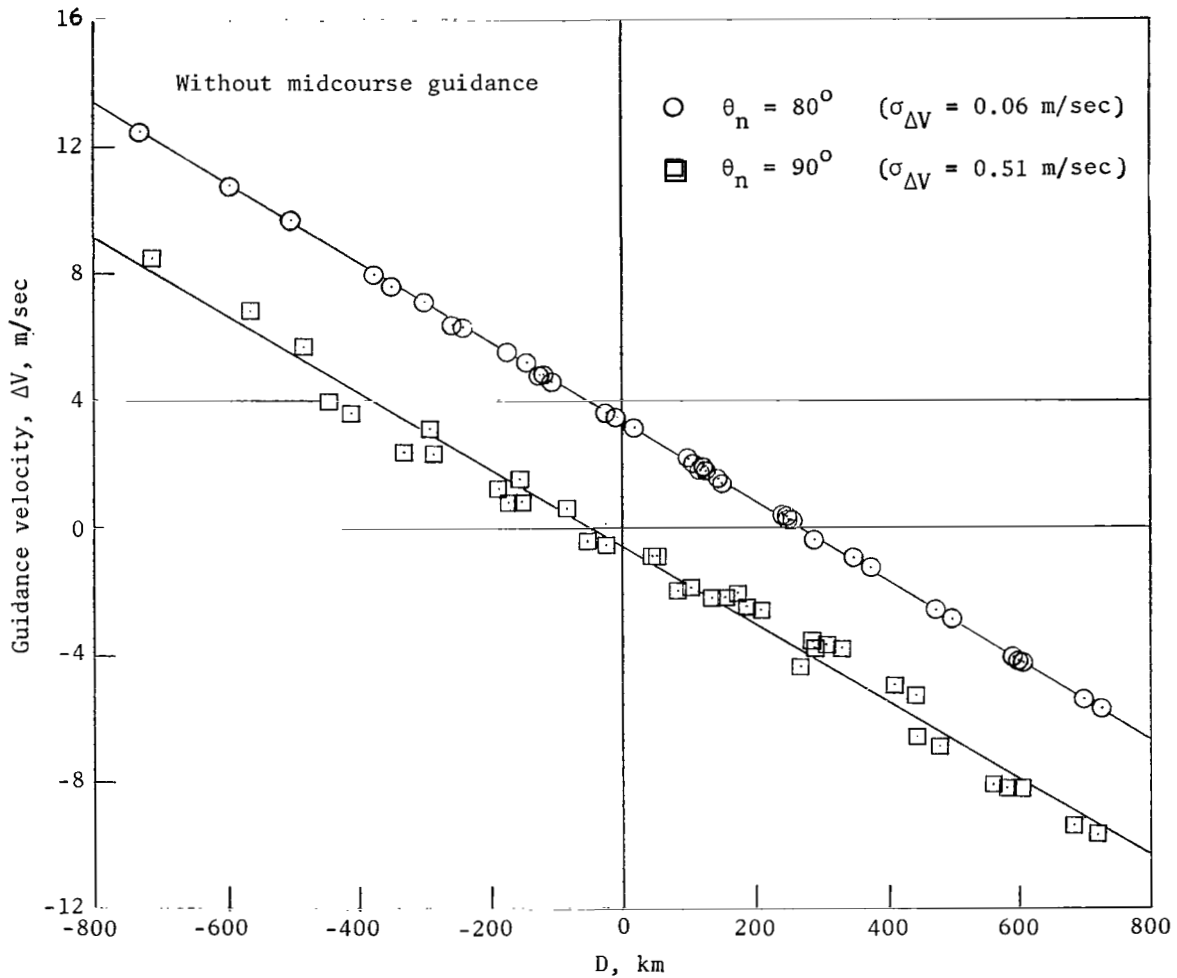


Figure 17.- Correlation of approach guidance velocity with deviation at $T_e = 17.4$ hours. $\lambda = \pm 90^\circ$; D is in nominal orbital plane. (Note staggered vertical scale.)

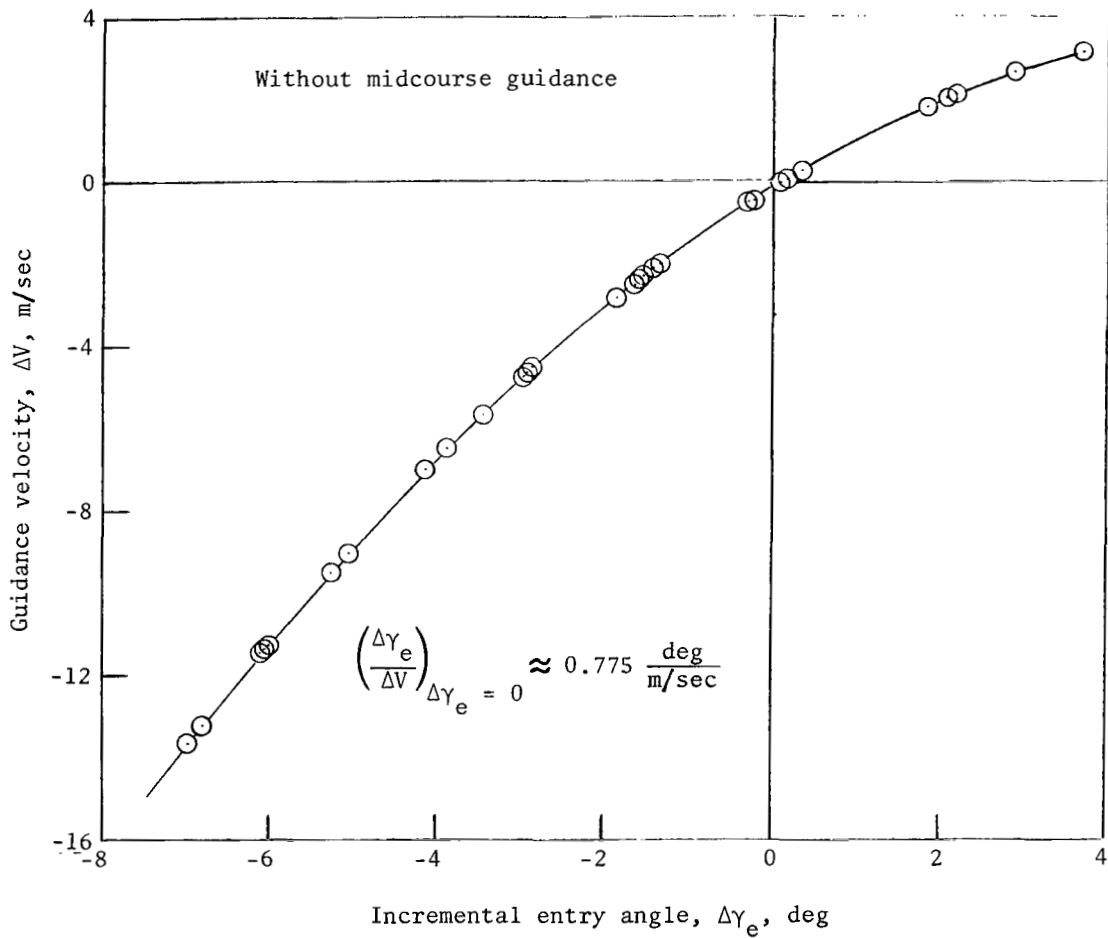


Figure 18.- Approach guidance velocity requirement as a function of incremental entry angle at nominal entry altitude. $\lambda = \pm 90^\circ$; $T_e = 9.4$ hours.

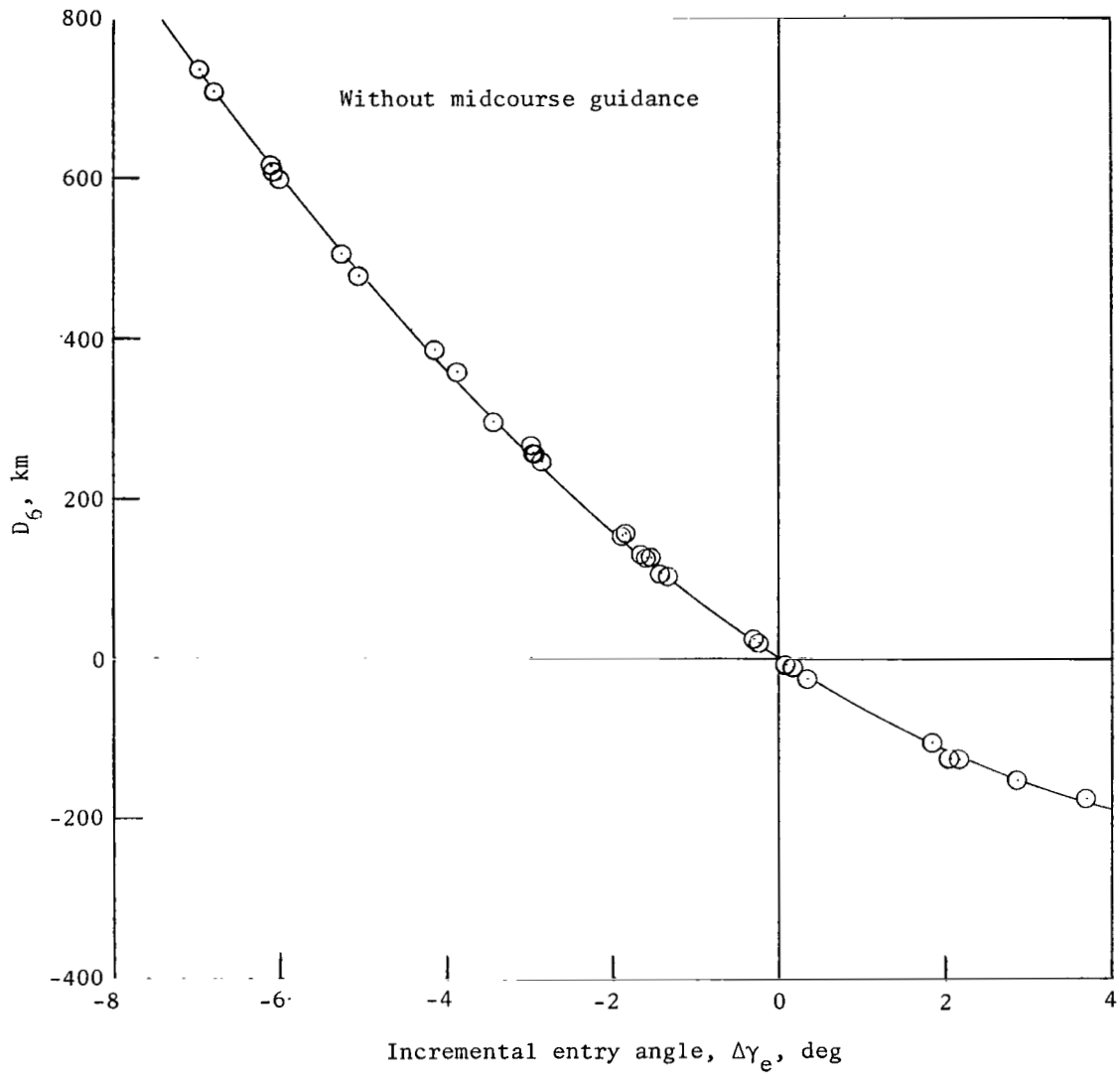


Figure 19.- Sensitivity of entry angle at nominal altitude with deviation D_6 at $T_e = 9.4$ hours. $\theta_n = 77^\circ$.

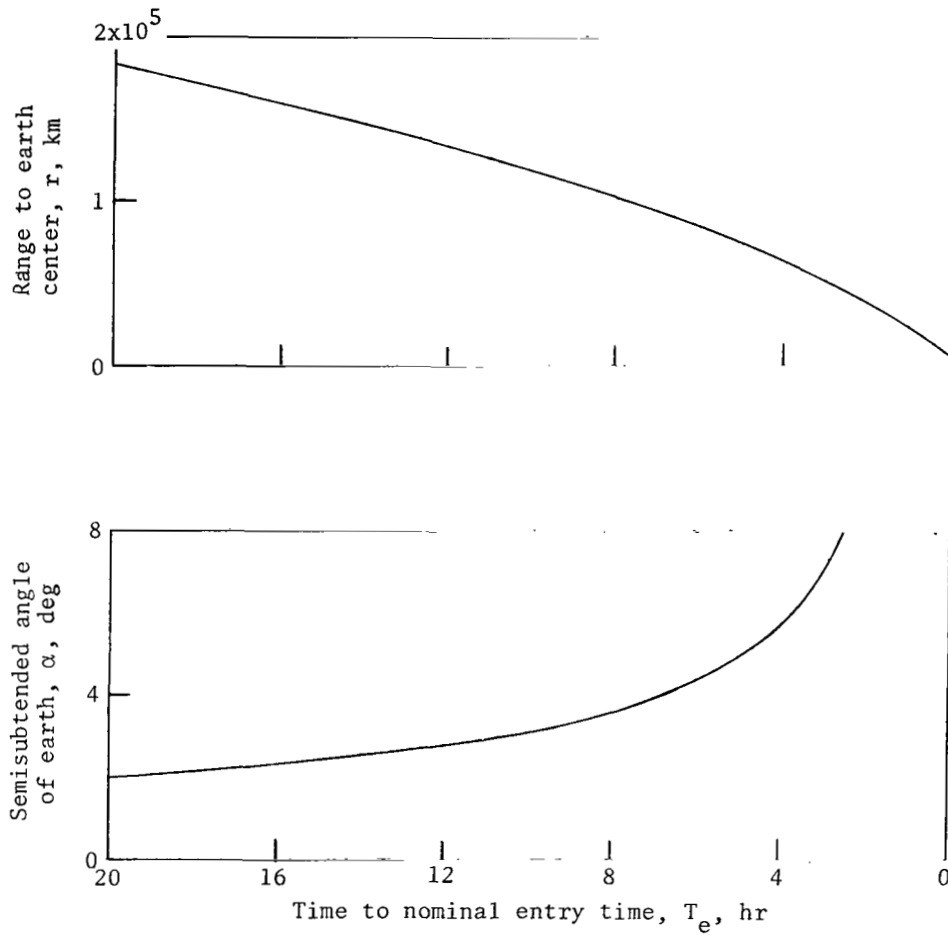


Figure 20.- Characteristics of nominal trajectory.

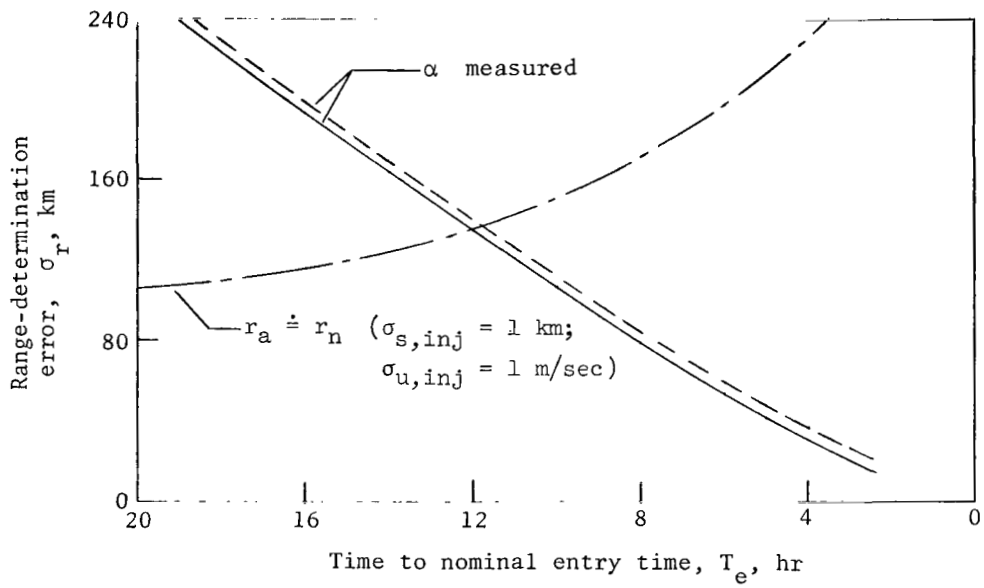


Figure 21.- Range-determination error. Measurement error $\sigma_\alpha = 10$ seconds of arc.
Dashed line includes effect of 2-km uncertainty in earth radius.

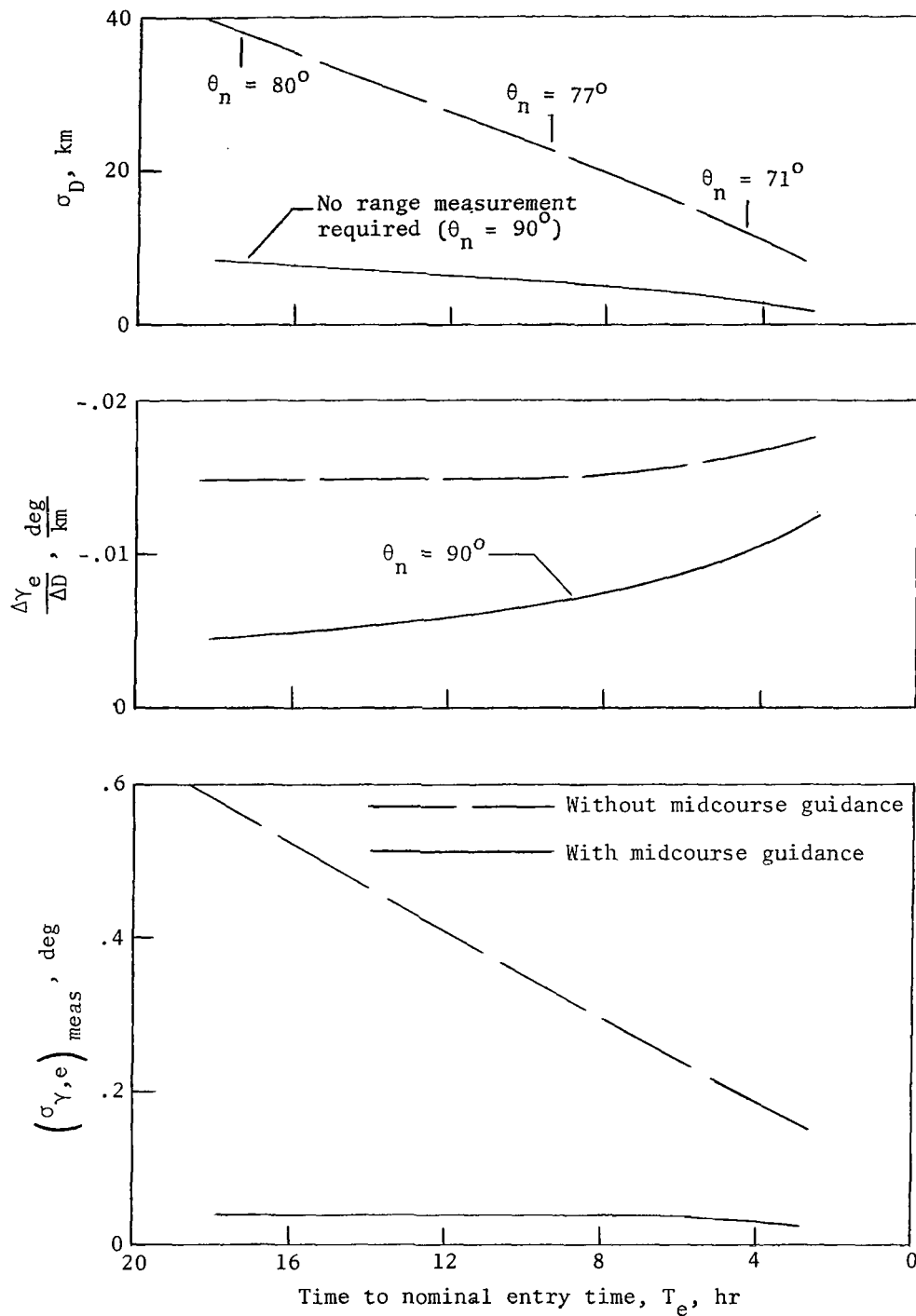


Figure 22.- Effect of measurement error on approach-guidance accuracy.
 $\sigma_R = 0$; measurement error $\sigma_\theta = 10$ seconds of arc.

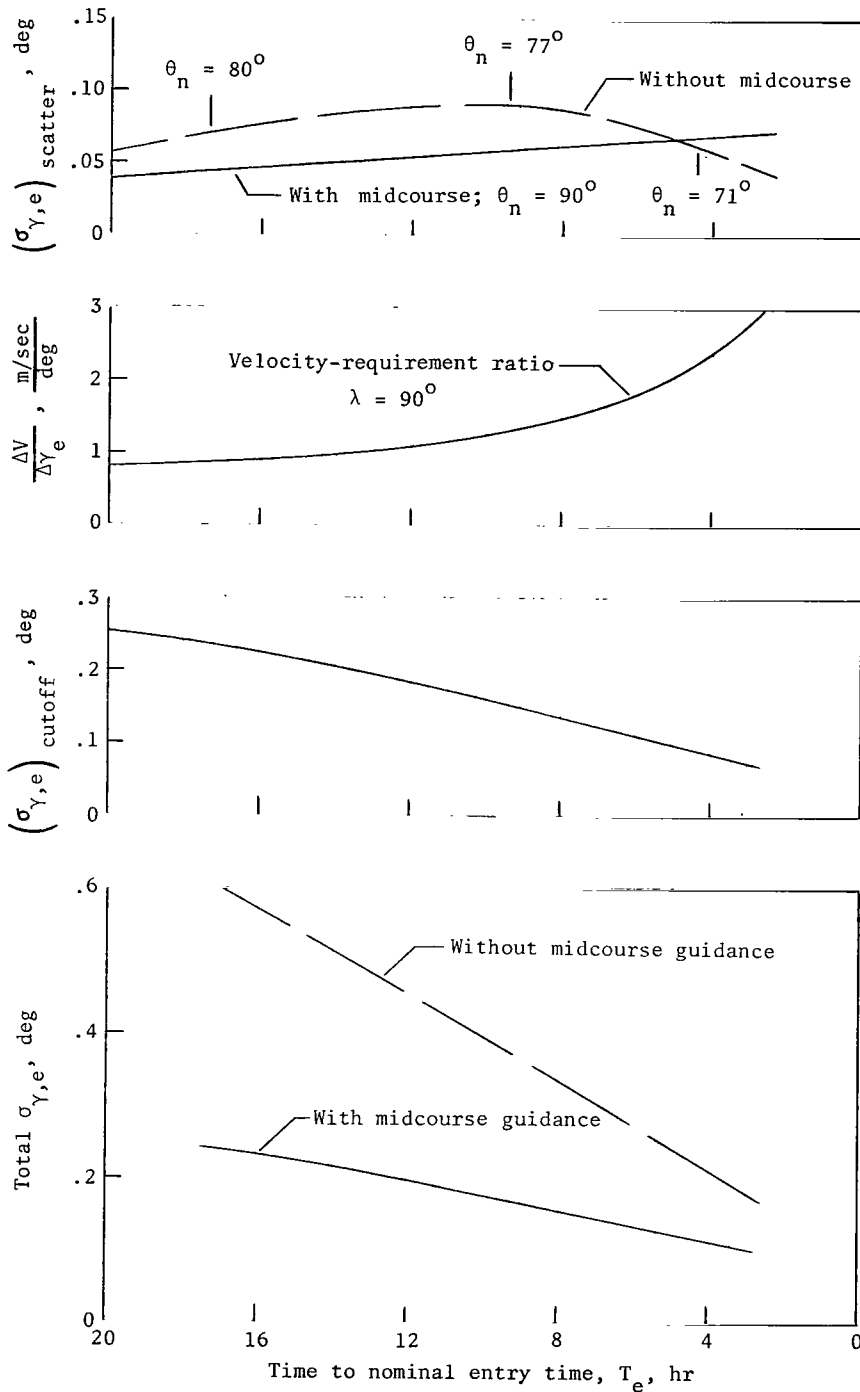


Figure 23.- Approach-guidance accuracy characteristics with effects of scatter error and maneuvering error included. The 1σ value of velocity-cutoff error is 0.2 m/sec.

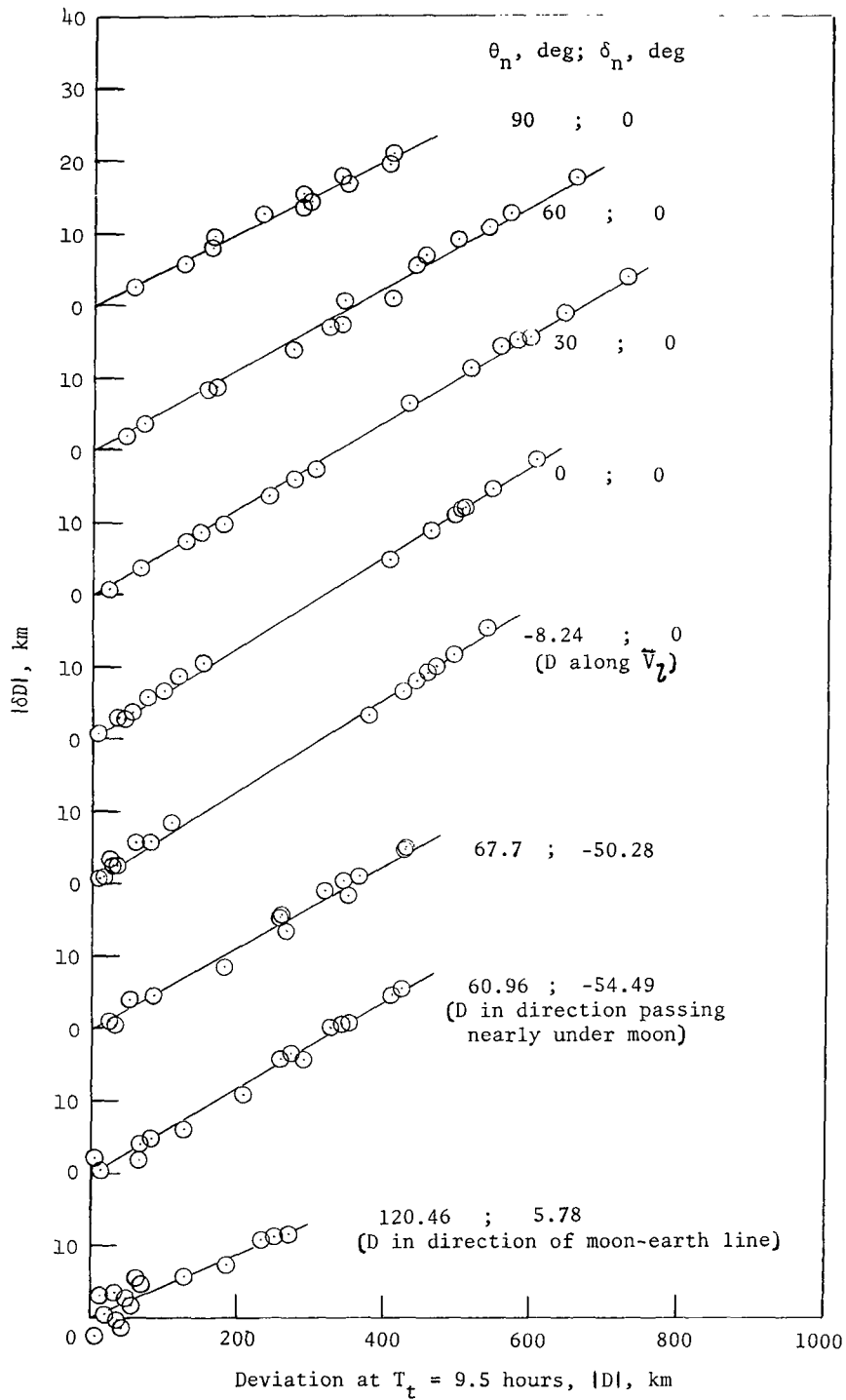


Figure 24.- Change in deviation from $T_t = 9.5$ hours to $T_t = 10$ hours for various perturbed transearth trajectories. D and δD agree in sign except for points below the zero line.

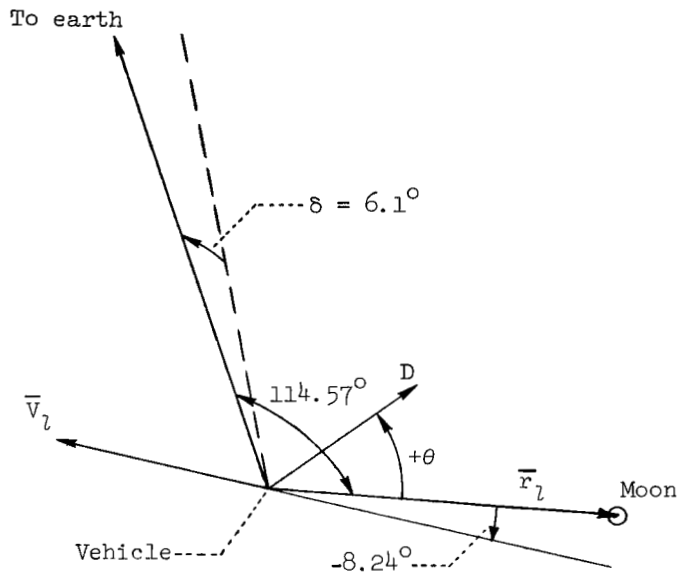


Figure 25.- Geometry in vehicle selenocentric orbital plane at 9.5 hours from transearth injection. Positive δ is in northerly direction from plane; θ is not necessarily in plane.

NATIONAL AERONAUTICS AND SPACE ADMINISTRATION
WASHINGTON, D. C. 20546
OFFICIAL BUSINESS
PENALTY FOR PRIVATE USE \$300

FIRST CLASS MAIL



POSTAGE AND FEES PAID
NATIONAL AERONAUTICS AND
SPACE ADMINISTRATION

001 001 C1 U 21 710716 S00903DS
DEPT OF THE AIR FORCE
WEAPONS LABORATORY /WLGL/
ATTN: E LOU BOWMAN, CHIEF TECH LIBRARY
KIRTLAND AFB NM 87117

POSTMASTER: If Undeliverable (Section 158
Postal Manual) Do Not Return

"The aeronautical and space activities of the United States shall be conducted so as to contribute . . . to the expansion of human knowledge of phenomena in the atmosphere and space. The Administration shall provide for the widest practicable and appropriate dissemination of information concerning its activities and the results thereof."

— NATIONAL AERONAUTICS AND SPACE ACT OF 1958

NASA SCIENTIFIC AND TECHNICAL PUBLICATIONS

TECHNICAL REPORTS: Scientific and technical information considered important, complete, and a lasting contribution to existing knowledge.

TECHNICAL NOTES: Information less broad in scope but nevertheless of importance as a contribution to existing knowledge.

TECHNICAL MEMORANDUMS: Information receiving limited distribution because of preliminary data, security classification, or other reasons.

CONTRACTOR REPORTS: Scientific and technical information generated under a NASA contract or grant and considered an important contribution to existing knowledge.

TECHNICAL TRANSLATIONS: Information published in a foreign language considered to merit NASA distribution in English.

SPECIAL PUBLICATIONS: Information derived from or of value to NASA activities. Publications include conference proceedings, monographs, data compilations, handbooks, sourcebooks, and special bibliographies.

TECHNOLOGY UTILIZATION PUBLICATIONS: Information on technology used by NASA that may be of particular interest in commercial and other non-aerospace applications. Publications include Tech Briefs, Technology Utilization Reports and Technology Surveys.

Details on the availability of these publications may be obtained from:

SCIENTIFIC AND TECHNICAL INFORMATION OFFICE

NATIONAL AERONAUTICS AND SPACE ADMINISTRATION

Washington, D.C. 20546